Mathematical Tripos Part III Essay #75 (colour in electronic version)
Submitted 5th May 2017, updated 26th August 2017

Primordial Gravitational Waves from Cosmic Inflation

Mike S. Wang
DAMTP, University of Cambridge

Abstract. Cosmic inflation generates primordial gravitational waves (PGWs) through the same physical process that seeds all structure formation in the observable universe. We will demonstrate this mechanism in detail and relate it to the distinctive signatures PGWs could leave in the observable temperature anisotropies and polarisation of the cosmic microwave background (CMB). The detection of primordial gravitational waves is of great significance to validating and understanding inflationary physics, and we shall see why CMB polarisation offers a promising path. In the end, we will remark on the unique observational challenges and prospects of probing primordial gravitational waves in future experiments.

Keywords. Inflation, primordial gravitational waves (theory), gravitational waves and CMBR polarisation, power spectrum, gravitational waves / experiments.

Contents

I A Brief Overview

Technological advances in the past decade have ushered cosmology into an exciting era where theory and observations are directly confronted. Increasing precision by orders of magnitude in measurements of the cosmological parameters enables us to further probe conditions of the very early universe, thus deepening our understanding of fundamental physics. Currently the inflation paradigm has been successful in solving numerous puzzles in the standard Big Bang cosmology, such as the horizon problem, the flatness problem and the relic problem; however, evidence for its happening is yet to be found, and its energy scales to be determined [1].

The cosmic microwave background (CMB) is a powerful utility for discovering evidence of inflation; primordial gravitational waves (PGWs) generated from the same inflationary mechanism that seeds large structure formation leave observable imprints in the CMB. In Sec. II and Sec. III, we will explore in detail this mechanism and the related physical observables. Sec. IV demonstrates why CMB polarisation offers a promising route for PGW detections. The significance of such a detection for understanding fundamental physics in the very early universe is discussed in Sec. V, before we finally remark on the obstacles as well as positive outlooks of future experimental efforts in Sec. VI.

Unless otherwise noted, the conventions adopted in this paper are: 1) mostly-plus Lorentzian signature $(-,+,+,+)$; 2) natural units in which $\hbar = c = 1$, and the reduced Planck mass $M_{\rm Pl} = 1/\sqrt{8\pi G}$; 3) Latin alphabet for spatial indices and Greek alphabet for spacetime indices; 4) the Hubble parameter denoted by $H \equiv \dot{a}/a$ and the comoving Hubble parameter denoted by $\mathcal{H} \equiv \dot{a}$, with a being the scale factor.

II The Inflation Paradigm and Generation of Gravitational Waves

The theory of inflation *postulates* a brief period (within 10^{-34} s) of quasi-exponential *accelerated expansion* during which the scale factor increased by over 60 e-folds. The intense expansion is sourced by a negative pressure component in energy-momentum of the matter contents, and drives the universe towards almost perfect homogeneity, isotropy and flatness [2].

A key prediction of inflation, which does not exist in non-inflationary physics, is the generation of primordial gravitational waves resulting from tensor perturbations in the geometry of the very early universe; as such, PGWs are often said to be a "smoking gun" for validating the inflation theory [1].

II.1 Dynamics of single-field slow-roll inflation

As an entry point, we first consider a simple model in which inflation is driven by a single scalar field $\phi(t,\mathbf{x})$, known as the *inflaton*, with an interaction potential $V(\phi)$. Its energy density and pressure

$$\begin{aligned} \rho \equiv -T^0{}_0 &= \frac{1}{2}\dot{\phi}^2 + V(\phi), \\ P \equiv \frac{1}{3}T^i{}_i &= \frac{1}{2}\dot{\phi}^2 - V(\phi) \end{aligned} \tag{1}$$

can be calculated from the energy-momentum tensor

$$T_{\mu\nu} = \partial_\mu\phi\partial_\nu\phi - g_{\mu\nu}\left[\frac{1}{2}\partial^\lambda\phi\partial_\lambda\phi + V(\phi)\right]. \tag{2}$$

The Friedman equations

$$H^2 = \frac{1}{3M_{\rm Pl}^2}\rho, \tag{3}$$

$$\dot{H} + H^2 = -\frac{1}{6M_{\rm Pl}^2}(\rho + 3P) \tag{4}$$

are obtained from the Einstein field equation applied to the most general metric for an expanding universe assuming the *cosmological principle*—the *Friedmann–Lemaître–Robertson–Walker (FLRW) metric*. The unperturbed form of the FLRW metric can be taken as

$$\mathrm{d}s^2 = a(\tau)^2\left(-\mathrm{d}\tau^2 + \mathrm{d}\mathbf{x}\cdot\mathrm{d}\mathbf{x}\right). \tag{5}$$

From the Friedman equations, it is easy to see that the condition of inflation $\ddot{a} > 0$ is equivalent to $\dot{\phi}^2 < V(\phi)$. Further, differentiating Eqn. (3) with respect to time and employing Eqns. (1) and (4) lead to the *Klein–Gordon equation* governing the scalar inflaton dynamics

$$\ddot{\phi} + 3H\dot{\phi} + V_{,\phi} = 0 \tag{6}$$

where the subscript "$,\phi$" denotes ϕ-derivatives.

A simple, approximate case is the *slow-roll* model: the inflaton rolls down a region of small gradients in the potential with its potential energy dominating over kinetic energy, $|V| \gg \dot{\phi}^2$. Differentiating this condition with respect to time shows that this process is sustained if

$$\left|\ddot{\phi}\right| \ll \left|V_{,\phi}\right|.$$

Two *slow-roll parameters*, defined for general inflationary models, gauge this process

$$\epsilon := -\frac{\mathrm{d}\ln H}{\mathrm{d}\ln a} \equiv -\frac{\dot{H}}{H^2}, \qquad \eta := \frac{\mathrm{d}\ln \epsilon}{\mathrm{d}\ln a} \equiv \frac{\dot{\epsilon}}{H\epsilon}. \tag{7}$$

In the slow-roll model, these parameters are both $\ll 1$ in magnitude

$$\epsilon \equiv \frac{1}{2M_{\mathrm{Pl}}^2}\frac{\dot{\phi}^2}{H^2} \approx \epsilon_V \equiv \frac{M_{\mathrm{Pl}}^2}{2}\left(\frac{V_{,\phi}}{V}\right)^2, \qquad \eta \approx 4\epsilon_V - 2\eta_V, \quad \eta_V \equiv M_{\mathrm{Pl}}^2\frac{V_{,\phi\phi}}{V}. \tag{8}$$

Here ϵ_V, η_V are the *potential slow-roll parameters* which are often more convenient to use in slow-roll scenarios [2]. Their linear relations above with the slow-roll parameters follow from the Friedman equation (3) and the Klein–Gordon equation (6) in the slow-roll approximation.

II.2 Quantum fluctuations and the primordial power spectrum

The background inflaton field $\bar{\phi}(t)$ is only time-dependent and acts as a "clock" during the inflationary period. However, as quantum effects are important in the early universe, by the uncertainty principle the inflaton field locally fluctuates around its background value, $\phi(t,\mathbf{x}) = \bar{\phi}(t) + \delta\phi(t,\mathbf{x})$. This means different amounts of inflation occur at different locations in spacetime, leading to density inhomogeneities in the universe from which structure ultimately forms.

We start our quantisation procedure from the *inflaton action* [2] assuming the unperturbed FLRW metric (5)

$$\begin{aligned} S &= \int \mathrm{d}\tau\, \mathrm{d}^3x\, \sqrt{-g}\left[-\frac{1}{2}g^{\mu\nu}\partial_\mu\phi\partial_\nu\phi - V(\phi)\right] \\ &= \int \mathrm{d}\tau\, \mathrm{d}^3x\, \frac{1}{2}a^2\left[\phi'^2 - \left(\boldsymbol{\nabla}\phi\right)^2 - 2a^2V(\phi)\right] \end{aligned} \tag{9}$$

where we denote the derivative of ϕ with respect to conformal time τ by ϕ' to distinguish from the derivative $\dot{\phi}$ with respect to cosmic time t. Introducing the field re-definition $f(\tau,\mathbf{x}) = a(\tau)\,\delta\phi(\tau,\mathbf{x})$ and ignoring metric fluctuations in the inflationary background[1], we expand the action (9) to second order

$$\begin{aligned} {}^{(2)}S &= \int \mathrm{d}\tau\, \mathrm{d}^3x\, \frac{1}{2}a^2\left[\left(\frac{f'}{a} - \frac{\mathcal{H}f}{a}\right)^2 - \left(\frac{\boldsymbol{\nabla}f}{a}\right)^2 - a^2V_{,\phi\phi}\left(\frac{f}{a}\right)^2\right] \\ &= \frac{1}{2}\int \mathrm{d}\tau\, \mathrm{d}^3x\left[f'^2 - \left(\boldsymbol{\nabla}f\right)^2 - \mathcal{H}(f^2)' + (\mathcal{H}^2 - a^2V_{,\phi\phi})f^2\right] \\ &= \frac{1}{2}\int \mathrm{d}\tau\, \mathrm{d}^3x\left[f'^2 - \left(\boldsymbol{\nabla}f\right)^2 + \left(\mathcal{H}' + \mathcal{H}^2 - a^2V_{,\phi\phi}\right)f^2\right] \\ &= \frac{1}{2}\int \mathrm{d}\tau\, \mathrm{d}^3x\left[f'^2 - \left(\boldsymbol{\nabla}f\right)^2 + \left(\frac{a''}{a} - a^2V_{,\phi\phi}\right)f^2\right]. \end{aligned}$$

We note that in slow-roll approximations, $H \approx$ const. and $\rho \approx V$, so by Eqn. (3)

$$\frac{a''}{a} \approx 2a^2H^2 \approx \frac{2}{3\eta_V}a^2V_{,\phi\phi} \gg a^2V_{,\phi\phi}$$

as $\eta \ll 1$. Therefore,

$${}^{(2)}S \approx \int \mathrm{d}\tau\, \mathrm{d}^3x\, \frac{1}{2}\left[f'^2 - \left(\boldsymbol{\nabla}f\right)^2 + \frac{a''}{a}f^2\right]. \tag{10}$$

By considering the associated Euler–Lagrange equation for the Lagrangian

$$\mathcal{L} = \frac{1}{2}\left[f'^2 - \left(\boldsymbol{\nabla}f\right)^2 + \frac{a''}{a}f^2\right] \tag{11}$$

we arrive at the *Mukhanov–Sasaki equation*

$$f'' - \nabla^2 f - \frac{a''}{a}f^2 = 0. \tag{12}$$

In *canonical quantisation*, $f(\tau,\mathbf{x})$ as well as its conjugate momentum $\pi(\tau,\mathbf{x}) \equiv \partial\mathcal{L}\big/\partial f' = f'$ are promoted to be operators obeying the *equal-time* canonical commutation relation (CCR)

$$\left[\hat{f}(\tau,\mathbf{x}), \hat{\pi}(\tau,\mathbf{x}')\right] = \mathrm{i}\delta(\mathbf{x}-\mathbf{x}'). \tag{13}$$

[1] A more rigorous treatment can be found in [3], but for our purposes the analysis below is sufficient for de Sitter expansion.

We expand $\hat{f}(\tau,\mathbf{x})$ and $\hat{\pi}(\tau,\mathbf{x})$ in Fourier space as

$$\begin{aligned}\hat{f}(\tau,\mathbf{x}) &= \int \frac{\mathrm{d}^3k}{(2\pi)^{3/2}}\left(f_k^* a_{\mathbf{k}}^\dagger \mathrm{e}^{-\mathrm{i}\mathbf{k}\cdot\mathbf{x}} + f_k a_{\mathbf{k}} \mathrm{e}^{\mathrm{i}\mathbf{k}\cdot\mathbf{x}}\right),\\ \hat{\pi}(\tau,\mathbf{x}) &= \int \frac{\mathrm{d}^3k}{(2\pi)^{3/2}}\left(f_k'^* a_{\mathbf{k}}^\dagger \mathrm{e}^{-\mathrm{i}\mathbf{k}\cdot\mathbf{x}} + f_k' a_{\mathbf{k}} \mathrm{e}^{\mathrm{i}\mathbf{k}\cdot\mathbf{x}}\right)\end{aligned} \tag{14}$$

where $a_{\mathbf{k}}$, $a_{\mathbf{k}}^\dagger$ are the time-independent annihilation and creation operators for each mode satisfying

$$\left[a_{\mathbf{k}}, a_{\mathbf{k}'}^\dagger\right] = \delta(\mathbf{k}-\mathbf{k}'), \tag{15}$$

and f_k satisfies Eqn. (12) in Fourier space

$$f_k'' + \omega_k^2(\tau) f_k = 0 \tag{16}$$

with $\omega_k^2 := k^2 - a''/a$, $k \equiv |\mathbf{k}|$. Now Eqns. (13) and (15) demand that the Wronskian

$$\mathcal{W}(f_k^*, f_k) \equiv f_k^* f_k' - f_k f_k^{*\prime} = -\mathrm{i}. \tag{17}$$

Since the expansion is quasi-*de Sitter* during inflation, i.e. $a \approx \mathrm{e}^{Ht}$ and $H \approx$ const., we have

$$\tau(t) = -\int_t^\infty \frac{\mathrm{d}t'}{a(t')} \approx -\int_t^\infty \mathrm{d}t'\, \mathrm{e}^{-Ht'} = -\frac{1}{aH},$$

and Eqn. (16) specialises to

$$f_k'' + \left(k^2 - \frac{2}{\tau^2}\right) f_k = 0. \tag{18}$$

The exact solution to this is given by

$$f_k(\tau) = A\frac{\mathrm{e}^{-\mathrm{i}k\tau}}{\sqrt{2k}}\left(1 - \frac{\mathrm{i}}{k\tau}\right) + B\frac{\mathrm{e}^{\mathrm{i}k\tau}}{\sqrt{2k}}\left(1 + \frac{\mathrm{i}}{k\tau}\right),$$

but we must choose the positive-frequency solution suitably normalised such that $\lim_{\tau\to-\infty} f_k(\tau) = \mathrm{e}^{-\mathrm{i}k\tau}/\sqrt{2k}$. This ensures that Eqn. (17) is satisfied and the vacuum state is the ground state of the Hamiltonian [2]. Hence we adopt

$$f_k = \frac{\mathrm{e}^{-\mathrm{i}k\tau}}{\sqrt{2k}}\left(1 - \frac{\mathrm{i}}{k\tau}\right). \tag{19}$$

We are ready now to determine the *power spectrum* for a physical observable q

$$\left\langle q(\mathbf{k}) q^*(\mathbf{k}')\right\rangle \equiv \frac{2\pi^2}{k^3}\mathcal{P}_q(k)\delta(\mathbf{k}-\mathbf{k}') \tag{20}$$

in the case of the *inflaton field* $q = \delta\phi = f/a$. Using Eqn. (14), we can calculate the zero-point fluctuation

$$\begin{aligned}&\left\langle 0\middle|\hat{f}(\tau,\mathbf{0})\hat{f}^\dagger(\tau,\mathbf{0})\middle|0\right\rangle\\ &\quad= \int \frac{\mathrm{d}^3k}{(2\pi)^{3/2}}\frac{\mathrm{d}^3k'}{(2\pi)^{3/2}} f_k f_{k'}^* \left\langle 0\middle|\left[a_{\mathbf{k}}, a_{\mathbf{k}'}^\dagger\right]\middle|0\right\rangle\\ &\quad= \int \mathrm{d}\ln k\, \frac{k^3}{2\pi^2}\left|f_k\right|^2\end{aligned}$$

and read off $\mathcal{P}_f = \left(k^3/2\pi\right)\left|f_k(\tau)\right|^2$. By solution (19),

$$\begin{aligned}\mathcal{P}_{\delta\phi}(k) &= a^{-2}\mathcal{P}_f(k)\\ &= (-H\tau)^2\frac{k^3}{2\pi^2}\frac{1}{2k}\left[1 + \frac{1}{(k\tau)^2}\right]\\ &= \left(\frac{H}{2\pi}\right)^2\left(1 + \frac{k^2}{a^2H^2}\right)\\ &\to \left(\frac{H}{2\pi}\right)^2\end{aligned} \tag{21}$$

on super-horizon scales $k \ll aH$.

Now we arrive at an important result: since H is slowly varying, we *approximate* the inflaton power spectrum by evaluating at *horizon crossing* $k = aH$

$$\mathcal{P}_{\delta\phi}(k) \approx \left(\frac{H_k}{2\pi}\right)^2, \quad \text{where} \quad H_k \equiv \frac{k}{a}. \tag{22}$$

II.3 Scalar, vector and tensor perturbations in the FLRW background

For later comparison and completeness, we will describe briefly scalar and vector perturbations as well as tensor perturbations in the FLRW background spacetime. The general perturbed FLRW metric takes the form

$$\begin{aligned}\mathrm{d}s^2 = a(\tau)^2\Big\{&-(1+2A)\,\mathrm{d}\tau^2 + 2B_i\,\mathrm{d}x^i\,\mathrm{d}\tau\\ &+ \left[(1+2C)\delta_{ij} + 2E_{ij}\right]\mathrm{d}x^i\,\mathrm{d}x^j\Big\}\end{aligned} \tag{23}$$

where E_{ij} is traceless, and spatial indices are raised and lowered using δ_{ij}.

Scalar perturbations — Scalar density inhomogeneities from cosmic inflation grow through gravitational instability, which explains large structure formation seen in the observable universe [4]. Gauge freedom allows us to push scalar perturbations into the curvature: in comoving gauge where $\delta\phi = 0$, the spatial metric

$$g_{ij} = a(t)^2\,\mathrm{e}^{2\tilde{\zeta}}\delta_{ij}; \tag{24}$$

$\tilde{\zeta}$ is the *gauge-invariant comoving curvature perturbation* ζ evaluated in this gauge. In spatially-flat gauge, ζ takes the form [2]

$$\zeta = -H\frac{\delta\phi}{\dot{\phi}}. \tag{25}$$

By comparing with the inflaton power spectrum (22), we find the scalar perturbation power spectrum

$$\mathcal{P}_\zeta = \frac{1}{2M_{\mathrm{Pl}}^2\epsilon}\left(\frac{H_k}{2\pi}\right)^2. \tag{26}$$

Scale-dependence of the power spectrum is measured by the *scalar spectral index*, or *tilt*,

$$n_s := 1 + \frac{\mathrm{d}\ln \mathcal{P}_\zeta}{\mathrm{d}\ln k} \tag{27}$$

where a value of unity corresponds to scale-invariance. The power spectrum could be approximated by a power-law with some reference scale [1] $k_\star$,

$$\mathcal{P}_\zeta(k) = A_s(k_\star)\left(\frac{k}{k_\star}\right)^{n_s-1}. \tag{28}$$

Vector perturbations — Primordial vector perturbations are negligible after inflation since they are associated with vorticity, which by conservation of angular momentum is diluted with the scale factor (see [5]).

[To avoid clustering of superscripts, we adopt the following convention in the context of tensor perturbations (gravitational waves): an overdot "˙" represents *derivatives with respect to the conformal time*, now denoted by η, rather than the cosmic time t.]

Tensor perturbations — Primordial gravitational waves are, mathematically speaking, tensor perturbations to the spacetime metric. In the FLRW background, we can write the perturbation as

$$\mathrm{d}s^2 = a(\eta)^2\left[-\mathrm{d}\eta^2 + \left(\delta_{ij} + h_{ij}\right)\mathrm{d}x^i\,\mathrm{d}x^j\right] \tag{29}$$

where h_{ij} is symmetric, traceless and transverse, i.e. $h^i{}_i = 0$ and $\partial_i h^i{}_j = 0$, since we can always absorb the other parts of the tensor into scalar or vector perturbations which decouple from true tensor perturbations at the linear order [1]. These conditions imply that h_{ij} has only two degrees of freedom, which we shall denote as the helicity $p = \pm 2$.

It is helpful to decompose h_{ij} in Fourier modes

$$h_{ij} = \sum_{p=\pm 2}\int \frac{\mathrm{d}^3k}{(2\pi)^{3/2}} h_{ij}^{(p)}(\eta,\mathbf{k})\,\mathrm{e}^{\mathrm{i}\mathbf{k}\cdot\mathbf{x}}. \tag{30}$$

For $\mathbf{k}$ along the z-axis, we choose a set of basis tensors

$$m^{(\pm 2)}(\hat{\mathbf{z}}) = \frac{1}{2}(\hat{\mathbf{x}} \pm \mathrm{i}\hat{\mathbf{y}}) \otimes (\hat{\mathbf{x}} \pm \mathrm{i}\hat{\mathbf{y}}) \tag{31}$$

satisfying the orthogonality and reality conditions [6]

$$m_{ij}^{(p)}(\hat{\mathbf{k}})\left[m^{(q)ij}(\hat{\mathbf{k}})\right]^* = \delta^{pq}, \tag{32}$$

$$\left[m_{ij}^{(p)}(\hat{\mathbf{k}})\right]^* = m_{ij}^{(-p)}(\hat{\mathbf{k}}) = m_{ij}^{(p)}(-\hat{\mathbf{k}}). \tag{33}$$

In such a basis, we have

$$h_{ij}^{(\pm 2)}(\eta,\mathbf{k}) = \frac{1}{\sqrt{2}} m_{ij}^{(\pm 2)}(\hat{\mathbf{k}}) h^{(\pm 2)}(\eta,\mathbf{k}). \tag{34}$$

As in the inflaton case, we start from the combined Einstein–Hilbert action and the matter action

$$S = \frac{M_{\mathrm{Pl}}^2}{2}\int \mathrm{d}^4x\,\sqrt{-g}R + \int \mathrm{d}^4x\,\sqrt{-g}\left[-\frac{1}{2}\partial_\mu\phi\partial^\mu\phi - V(\phi)\right] \tag{35}$$

where R is the Ricci scalar, and expand to second order to find

$${}^{(2)}S = \frac{M_{\mathrm{Pl}}^2}{8}\int \mathrm{d}\eta\,\mathrm{d}^3x\,a^2\left(\dot{h}_{ij}\dot{h}^{ij} - \partial_i h_{jk}\partial^i h^{jk}\right). \tag{36}$$

This laborious calculation can be found in Appendix A.

Using Eqns. (30), (32), (33) and (34), we could rewrite terms in the second order action in the Fourier space as follows

$$\begin{aligned}\int \mathrm{d}^3x\,\dot{h}_{ij}\dot{h}^{ij} &= \sum_{p,q=\pm 2}\int \frac{\mathrm{d}^3k}{(2\pi)^{3/2}}\frac{\mathrm{d}^3k'}{(2\pi)^{3/2}}\frac{1}{2}\dot{h}^{(p)}(\eta,\mathbf{k})\dot{h}^{(q)}(\eta,\mathbf{k}')m_{ij}^{(p)}(\hat{\mathbf{k}})m^{(q)ij}(\hat{\mathbf{k}}')\int \mathrm{d}^3x\,\mathrm{e}^{\mathrm{i}(\mathbf{k}+\mathbf{k}')\cdot\mathbf{x}} \\ &= \frac{1}{2}\sum_{p,q=\pm 2}\int \frac{\mathrm{d}^3k}{(2\pi)^{3/2}}\frac{\mathrm{d}^3k'}{(2\pi)^{3/2}}\dot{h}^{(p)}(\eta,\mathbf{k})\dot{h}^{(q)}(\eta,\mathbf{k}')m_{ij}^{(p)}(\hat{\mathbf{k}})m^{(q)ij}(\hat{\mathbf{k}}')(2\pi)^3\delta(\mathbf{k}+\mathbf{k}') \\ &= \frac{1}{2}\sum_{p=\pm 2}\int \mathrm{d}^3k\left[\dot{h}^{(p)}(\eta,\mathbf{k})\right]^2\end{aligned}$$

and similarly

$$\int \mathrm{d}^3x\,\partial_i h_{jk}\partial^i h^{jk} = -\frac{1}{2}\sum_{p=\pm 2}\int \mathrm{d}^3k\,k^2\left[h^{(p)}(\eta,\mathbf{k})\right]^2$$

so that

$${}^{(2)}S = \frac{M_{\mathrm{Pl}}^2}{16}\sum_{p=\pm 2}\int \mathrm{d}\eta\,\mathrm{d}^3k\,a^2\left[\left(\dot{h}^{(p)}\right)^2 + k^2\left(h^{(p)}\right)^2\right]. \tag{37}$$

By comparing Eqn. (37) with the action (9) in Fourier space, we see that following the same quantisation procedure with $\delta\phi \to (M_{\rm Pl}/\sqrt{8})h^{(p)}$ for each independently-evolving helicity state, one can derive the power spectrum as defined in the two-point correlator,

$$\left\langle h^{(p)}(\mathbf{k})\left[h^{(p)}(\mathbf{k}')\right]^*\right\rangle \equiv \frac{2\pi^2}{k^3}\mathcal{P}_h(k)\delta(\mathbf{k}-\mathbf{k}'), \tag{38}$$

to be (at horizon crossing)

$$\mathcal{P}_h(k) = \frac{8}{M_{\rm Pl}^2}\left(\frac{H_k}{2\pi}\right)^2. \tag{39}$$

As in the case of scalar perturbations, we can define the *tensor spectral index*

$$n_{\rm t} := \frac{{\rm d}\ln\mathcal{P}_h(k)}{{\rm d}\ln k} \tag{40}$$

so that the tensor perturbation power spectrum (39) can be approximated by a power law

$$\mathcal{P}_h(k) = A_{\rm t}(k_\star)\left(\frac{k}{k_\star}\right)^{n_{\rm t}} \tag{41}$$

in analogy with Eqn. (28).

II.3.1 A consistency condition

Comparing the scalar and tensor power spectra (26), (39) and their power-law approximations (28), (41), we see that the *tensor-to-scalar ratio*, defined below, is

$$r := \frac{A_{\rm t}}{A_{\rm s}} = 16\epsilon. \tag{42}$$

We shall see later the CMB polarisation measurements are sensitive to this value, and it contains critical information about inflationary physics [1].

We have, from Eqns. (7), (39) and (40),

$$\begin{aligned} n_{\rm t} &= \frac{{\rm d}\ln\mathcal{P}_h}{{\rm d}\ln a}\frac{{\rm d}\ln a}{{\rm d}\ln k} \\ &= 2\frac{{\rm d}\ln H}{{\rm d}\ln a}\left(\frac{{\rm d}\ln k}{{\rm d}\ln a}\right)^{-1}\Bigg|_{k=aH} \\ &= -2\epsilon(1-\epsilon)^{-1} \\ &\approx -2\epsilon \end{aligned} \tag{43}$$

where we have used $\ln k = \ln a + \ln H$ at horizon crossing, so ${\rm d}\ln k/{\rm d}\ln a = 1-\epsilon$. Therefore a *consistency condition* is obtained for *canonical single-field slow-roll* inflation

$$r \approx -8n_{\rm t}. \tag{44}$$

II.3.2 Evolution of gravitational waves

In the absence of anisotropic stress, the traceless part of the ij-component of the Einstein field equation gives

$$\ddot{h}^{(\pm 2)} + 2\mathcal{H}\dot{h}^{(\pm 2)} + k^2 h^{(\pm 2)} = 0 \tag{45}$$

with solutions $h^{(\pm 2)} \propto {\rm e}^{\pm {\rm i}k\eta}/a$. Details of the derivation may be found in Appendix B.

III CMB Signatures from Primordial Gravitational Waves

Observational and precision cosmology has been making remarkable leaps in recent times and since its discovery, the cosmic microwave background has been an indispensable utility directly probing the very early universe. Local fluctuations in physical properties such as temperature and density were imprinted into the CMB at the time of *recombination*, when photons decoupled from the primordial plasma and became essentially free-streaming, presenting an almost perfect blackbody thermal spectrum. Angular variance in CMB radiation thus encodes the information of perturbations generated during the hypothetical inflationary era, lending us insights into the geometry and matter contents of the early universe [7].

Two key observables of the CMB are the *temperature anisotropy* and *polarisation*. We will discuss the distinctive signatures of PGWs in these observables, and explain why the latter gives a particularly promising route in the detection of PGWs in the next section.

III.1 Temperature anisotropies from PGWs

III.1.1 Concepts and notions

The blackbody spectrum — The Lorentz-invariant distribution function of CMB photons in the phase space is isotropic and homogeneous in the rest frame, but Doppler-shifted relativistically for an observer with relative velocity $\mathbf{v}$ to the background

$$\bar{f}(p^\mu) \propto \frac{1}{\exp\left[E\gamma(1+\mathbf{e}\cdot\mathbf{v})/\bar{T}_{\rm CMB}\right]-1}$$

where $\mathbf{e}$ is the direction of the incoming photon and E its observed energy, $\gamma \equiv (1-\mathbf{v}\cdot\mathbf{v})^{-1/2}$, and $\bar{T}_{\rm CMB} \simeq 2.7255\,{\rm K}$ is the isotropic CMB temperature. This is a blackbody spectrum with temperature varying with

direction $\mathbf{e}$ as $T(\mathbf{e}) \approx \bar{T}_{\rm CMB}(1 - \mathbf{e}\cdot\mathbf{v}), |\mathbf{v}| \ll 1$: we see here a dipole anisotropy—which along with *kinematic* quadrupole and multipole anisotropies at order $|\mathbf{v}|^2$ or higher—must be subtracted to give the *cosmological* anisotropies [6].

Optical depth and visibility — Along a *line of sight* $\mathbf{x} = \mathbf{x}_0 - (\eta_0 - \eta)\mathbf{e}$ between conformal times η and η_0, where the observation takes place at position $\mathbf{x}_0$, the optical depth is defined by

$$\tau := \int_\eta^{\eta_0} \mathrm{d}\eta\, a\bar{n}_{\rm e}\sigma_{\rm T} \tag{46}$$

and the visibility function is defined by

$$g(\eta) := -\dot{\tau}\,\mathrm{e}^{-\tau}. \tag{47}$$

Here $\mathrm{e}^{-\tau}$ is interpreted as the probability that a photon does *not* get scattered in the interval (η, η_0), and $g(\eta)$ is the probability density that a photon last-scattered at time η. They satisfy the integral relation [6]

$$\int_\eta^{\eta_0} \mathrm{d}\eta'\, g(\eta') = 1 - \mathrm{e}^{-\tau(\eta)}. \tag{48}$$

Rotations of a random field — Rotational transformations of a scalar random field $f(\hat{\mathbf{n}})$ on the sphere can be performed by acting on the spherical multipole coefficients $f_{\ell m}$ via the Wigner D-matrices. The relevant mathematics is found in Appendix C.

Angular power spectrum — The two-point correlator of a scalar random field $f(\hat{\mathbf{n}})$ is rotationally-invariant if [7]

$$\left\langle f_{\ell m} f^*_{\ell' m'} \right\rangle = C_\ell \delta_{\ell\ell'}\delta_{mm'} \tag{49}$$

where C_ℓ is the angular power spectrum associated with the random field f.

III.1.2 The Boltzmann equation for anisotropies

In what follows in this section, it is useful to express 3-vectors in terms of an orthonormal tetrad with components $(\mathcal{E}_0)^\mu$, $(\mathcal{E}_i)^\mu$ such that

$$g_{\mu\nu}(\mathcal{E}_0)^\mu(\mathcal{E}_0)^\nu = -1, \quad g_{\mu\nu}(\mathcal{E}_0)^\mu(\mathcal{E}_i)^\nu = 0,$$
$$g_{\mu\nu}(\mathcal{E}_i)^\mu(\mathcal{E}_j)^\nu = \delta_{ij}.$$

We denote the tetrad components of the direction of propagation vector $\mathbf{e}$ by $e^{\hat{\imath}}$, then the 4-momentum of a photon with energy E is

$$\left(E, p^{\hat{\imath}}\right) = \frac{\epsilon}{a}\left(1, e^{\hat{\imath}}\right) \tag{50}$$

where $\epsilon \equiv aE$ is the comoving photon energy.

We write

$$f(\eta, \mathbf{e}, \mathbf{x}, \epsilon) = \bar{f}(\epsilon)\left[1 - \Theta(\eta, \mathbf{x}, \mathbf{e})\frac{\mathrm{d}\ln\bar{f}}{\mathrm{d}\ln\epsilon}\right] \tag{51}$$

where Θ is the *fractional temperature fluctuation.* On physical grounds

$$\left.\frac{\mathrm{d}f}{\mathrm{d}\eta}\right|_{\rm path} = \left.\frac{\mathrm{d}f}{\mathrm{d}\eta}\right|_{\rm scatt.},$$

where the LHS is a total derivative along the photon path, and the RHS describes scattering effects. This leads to the *linearised Boltzmann equation* for $\Theta(\eta, \mathbf{x}, \mathbf{e})$

$$\frac{\partial\Theta}{\partial\eta} + \mathbf{e}\cdot\boldsymbol{\nabla}\Theta - \frac{\mathrm{d}\ln\epsilon}{\mathrm{d}\eta} = -a\bar{n}_{\rm e}\sigma_{\rm T}\Theta + a\bar{n}_{\rm e}\sigma_{\rm T}\mathbf{e}\cdot\mathbf{v}_{\rm b}$$
$$+ \frac{3a\bar{n}_{\rm e}\sigma_{\rm T}}{16\pi}\int \mathrm{d}\hat{\mathbf{m}}\,\Theta(\hat{\mathbf{m}})\left[1 + (\mathbf{e}\cdot\mathbf{m})^2\right] \tag{52}$$

where at linear order $\mathrm{d}/\mathrm{d}\eta = \partial/\partial\eta + \mathbf{e}\cdot\boldsymbol{\nabla}$ along a line of sight, $\bar{n}_{\rm e}$ is the average electron density, $\sigma_{\rm T}$ is the cross-section for Thomson scattering and $\mathbf{v}_{\rm b}$ is the velocity of baryons and electrons tightly coupled by Coulomb scattering [6].

Multipole expansion and normal modes — We can expand the fractional temperature fluctuation in Fourier space in the basis of the Legendre polynomials $P_\ell(x)$

$$\Theta(\eta, \mathbf{k}, \mathbf{e}) = \sum_{\ell\geqslant 0}(-\mathrm{i})^\ell\Theta_\ell(\eta, \mathbf{k})P_\ell(\hat{\mathbf{k}}\cdot\mathbf{e}), \tag{53}$$

or in the basis of the spherical harmonics

$$\Theta(\eta, \mathbf{k}, \mathbf{e}) = \sum_{\ell, m}\Theta_{\ell m}(\eta, \mathbf{k})Y_{\ell m}(\mathbf{e}). \tag{54}$$

Then by the addition formula [6]

$$P_\ell(\hat{\mathbf{k}}\cdot\mathbf{e}) = \sum_{|m|\leqslant\ell}\frac{4\pi}{2\ell+1}Y^*_{\ell m}(\hat{\mathbf{k}})Y_{\ell m}(\mathbf{e})$$

we have

$$\Theta_{\ell m}(\eta, \mathbf{k}) = (-\mathrm{i})^\ell\frac{4\pi}{2\ell+1}\Theta_\ell(\eta, \mathbf{k})Y^*_{\ell m}(\hat{\mathbf{k}}). \tag{55}$$

III.1.3 Linear anisotropies from gravitational waves

We will temporarily suppress the polarisation label (p), $p = \pm 2$, for readability. It is useful to work in an orthonormal tetrad, whose components are given by

$$(\mathcal{E}_0)^\mu = a^{-1}\delta^\mu_0, \quad (\mathcal{E}_i)^\mu = a^{-1}\left(\delta^\mu_i - \frac{1}{2}h_i{}^j\delta^\mu_j\right). \tag{56}$$

The time-component of the geodesic equation at linear order, for the metric (29), gives then an equation [7] satisfied by ϵ (see Appendix D)

$$\frac{1}{\epsilon}\frac{\mathrm{d}\epsilon}{\mathrm{d}\eta} + \frac{1}{2}\dot{h}_{ij}e^{\hat{i}}e^{\hat{j}} = 0. \tag{57}$$

For tensor perturbations, there are no perturbed scalars or 3-vectors, so $\mathbf{v}_\mathrm{b} = \mathbf{0}$ and the monopole

$$\int \mathrm{d}\hat{\mathbf{m}}\,\Theta(\hat{\mathbf{m}}) = 0.$$

Using Eqn. (57) and the integrating factor $\mathrm{e}^{-\tau}$ in the linearised Boltzmann equation (52), we obtain

$$\frac{\mathrm{d}}{\mathrm{d}\eta}\left(\mathrm{e}^{-\tau}\Theta\right) = -\dot{\tau}\,\mathrm{e}^{-\tau}\Theta - \mathrm{e}^{-\tau}a\bar{n}_\mathrm{e}\sigma_\mathrm{T}\Theta - \frac{1}{2}\mathrm{e}^{-\tau}\dot{h}_{ij}e^{\hat{i}}e^{\hat{j}} = -\frac{1}{2}\mathrm{e}^{-\tau}\dot{h}_{ij}e^{\hat{i}}e^{\hat{j}}$$

which can be integrated to

$$\Theta(\eta_0,\mathbf{x}_0,\mathbf{e}) \approx -\frac{1}{2}\int_0^{\eta_0}\mathrm{d}\eta\;\mathrm{e}^{-\tau}\dot{h}_{ij}e^{\hat{i}}e^{\hat{j}}. \tag{58}$$

Note here we have 1) recognised $\dot{\tau} = -a\bar{n}_\mathrm{e}\sigma_\mathrm{T}$ from definition (46); 2) evaluated $\tau(\eta_0) = 0$, $\tau(0) = \infty$; and 3) *neglected the temperature quadrupole* at last-scattering on large scales as it has not had the time grow.

The physical interpretation of this is that $\dot{h}_{ij}$ is the *shear* of the gravitational waves and $\dot{h}_{ij}e^{\hat{i}}e^{\hat{j}}$ contributes to the temperature anisotropies as a local quadrupole, as h is traceless [6].

We shall now attempt to evaluate the integral expression. First take a Fourier mode of h_{ij} given in Eqn. (34) along the z-axis,

$$\begin{aligned}\dot{h}^{(\pm2)}_{ij}(\eta,k\hat{\mathbf{z}})e^{\hat{i}}e^{\hat{j}} &= \frac{1}{2\sqrt{2}}\dot{h}^{(\pm2)}(\eta,k\hat{\mathbf{z}})\left[(\hat{\mathbf{x}}\pm\mathrm{i}\hat{\mathbf{y}})\cdot\mathbf{e}\right]^2\\ &= \frac{1}{2\sqrt{2}}\dot{h}^{(\pm2)}(\eta,k\hat{\mathbf{z}})\sin^2\theta\,\mathrm{e}^{\pm2\mathrm{i}\phi}\\ &= \sqrt{\frac{4\pi}{15}}\dot{h}^{(\pm2)}(\eta,k\hat{\mathbf{z}})Y_{2\pm2}(\mathbf{e})\end{aligned} \tag{59}$$

where θ, ϕ are the spherical polar coordinates of $\mathbf{e}$, and we have recalled the explicit form of the $(l,m) = (2,\pm2)$ spherical harmonic

$$Y_{2\pm2}(\mathbf{e}) = \sqrt{\frac{15}{32\pi}}\,\mathrm{e}^{\pm2\mathrm{i}\phi}\sin^2\theta.$$

The contribution from the integrand in Eqn. (58) at a particular time $\eta = \eta_0 - \chi$, where χ is the comoving distance from the observer now, is modulated by a phase factor due to the spatial dependence of gravitational waves. After some algebraic manipulations with the Rayleigh expansion and the Wigner $3j$-symbols (see Appendix E), we have the result

$$\begin{aligned}\dot{h}^{(\pm2)}_{ij}(\eta,k\hat{\mathbf{z}})e^{\hat{i}}e^{\hat{j}}\,\mathrm{e}^{-\mathrm{i}k\chi\cos\theta} &= -\sqrt{\frac{\pi}{2}}\dot{h}^{(\pm2)}(\eta,k\hat{\mathbf{z}})\\ &\times\sum_\ell(-\mathrm{i})^\ell\sqrt{2\ell+1}\sqrt{\frac{(\ell+2)!}{(\ell-2)!}}\frac{j_\ell(k\chi)}{(k\chi)^2}Y_{\ell\pm2}(\mathbf{e}).\end{aligned} \tag{60}$$

We are now ready to extend this result to Fourier modes with $\mathbf{k}$ along a general direction by a rotation via the Wigner D-matrix

$$\begin{aligned}\dot{h}^{(\pm2)}_{ij}(\eta,\mathbf{k})e^{\hat{i}}e^{\hat{j}}\,\mathrm{e}^{-\mathrm{i}k\chi\hat{\mathbf{k}}\cdot\mathbf{e}} &= -\sqrt{\frac{\pi}{2}}\dot{h}^{(\pm2)}(\eta,\mathbf{k})\\ &\times\sum_{\ell,m}(-\mathrm{i})^\ell\sqrt{2\ell+1}\sqrt{\frac{(\ell+2)!}{(\ell-2)!}}\frac{j_\ell(k\chi)}{(k\chi)^2}\\ &\times D^\ell_{m\pm2}(\phi_\mathbf{k},\theta_\mathbf{k},0)Y_{\ell m}(\mathbf{e})\end{aligned} \tag{61}$$

where explicitly

$$D^\ell_{m\pm2}(\phi_\mathbf{k},\theta_\mathbf{k},0) = \sqrt{\frac{4\pi}{2\ell+1}}\,{}_{\mp2}Y^*_{\ell m}(\hat{\mathbf{k}}).$$

In analogy with Eqns. (54) and (55), we expand the fractional temperature fluctuation in spherical multipoles

$$\begin{aligned}\Theta_{\ell m}(\eta_0,\mathbf{x}_0) &= \frac{1}{\sqrt{2}}\sum_{p=\pm2}\int\frac{\mathrm{d}^3k}{(2\pi)^{3/2}}(-\mathrm{i})^\ell\Theta^{(p)}_\ell(\eta_0,\mathbf{k})\\ &\times\sqrt{\frac{4\pi}{2\ell+1}}D^\ell_{mp}(\phi_\mathbf{k},\theta_\mathbf{k},0)\,\mathrm{e}^{\mathrm{i}\mathbf{k}\cdot\mathbf{x}_0},\end{aligned} \tag{62}$$

$$\begin{aligned}\Theta^{(p)}_\ell(\eta_0,\mathbf{k}) &= \frac{2\ell+1}{4}\int_0^{\eta_0}\mathrm{d}\eta'\;\mathrm{e}^{-\tau}\dot{h}^{(p)}(\eta',\mathbf{k})\\ &\times\sqrt{\frac{(\ell+2)!}{(\ell-2)!}}\frac{j_\ell(k\chi)}{(k\chi)^2}\end{aligned} \tag{63}$$

where inside the integral $\chi = \eta_0 - \eta'$.

III.1.4 Angular power spectrum of temperature anisotropies

To make contact with observations, we shall now compute the two-point correlator for the temperature anisotropies induced by gravitational waves.

$$
\begin{aligned}
\left\langle \Theta_{\ell m}\Theta^*_{\ell' m'}\right\rangle &= \left(\frac{1}{\sqrt{2}}\right)^2 (-\mathrm{i})^{\ell}(-\mathrm{i})^{-\ell'}\sqrt{\frac{4\pi}{2\ell+1}}\sqrt{\frac{4\pi}{2\ell'+1}}\sum_{p,q=\pm 2}\int \frac{\mathrm{d}^3k}{(2\pi)^{3/2}}\frac{\mathrm{d}^3k'}{(2\pi)^{3/2}}\left\langle h^{(p)}(\mathbf{k})h^{(q)*}(\mathbf{k}')\right\rangle \\
&\qquad \times \frac{\Theta_\ell^{(p)}(\eta_0,\mathbf{k})}{h^{(p)}(\mathbf{k})}\frac{\Theta_\ell^{(q)}(\eta_0,\mathbf{k}')}{h^{(q)}(\mathbf{k}')} D^{\ell}_{mp}(\phi_{\mathbf{k}},\theta_{\mathbf{k}},0)D^{\ell'}_{m'q}(\phi_{\mathbf{k}'},\theta_{\mathbf{k}'},0)\,\mathrm{e}^{\mathrm{i}(\mathbf{k}-\mathbf{k}')\cdot\mathbf{x}_0} \\
&= \frac{(-\mathrm{i})^{\ell-\ell'}}{\sqrt{(2\ell+1)(2\ell'+1)}}\frac{1}{4\pi^2}\sum_{p,q=\pm 2}\int \mathrm{d}^3k\,\mathrm{d}^3k'\,\frac{2\pi^2}{k^3}\mathcal{P}_h(k)\delta(\mathbf{k}-\mathbf{k}')\delta^{pq} \\
&\qquad \times \frac{\Theta_\ell^{(p)}(\eta_0,\mathbf{k})}{h^{(p)}(\mathbf{k})}\frac{\Theta_\ell^{(q)}(\eta_0,\mathbf{k}')}{h^{(q)}(\mathbf{k}')} D^{\ell}_{mp}(\phi_{\mathbf{k}},\theta_{\mathbf{k}},0)D^{\ell'}_{m'q}(\phi_{\mathbf{k}'},\theta_{\mathbf{k}'},0)\,\mathrm{e}^{\mathrm{i}(\mathbf{k}-\mathbf{k}')\cdot\mathbf{x}_0} \\
&= \frac{(-\mathrm{i})^{\ell-\ell'}}{2\sqrt{(2\ell+1)(2\ell'+1)}}\sum_{p=\pm 2}\int \mathrm{d}\ln k\,\mathcal{P}_h(k)\left[\frac{\Theta_\ell^{(p)}(\eta_0,\mathbf{k})}{h^{(p)}(\mathbf{k})}\right]^2 \underbrace{\int \mathrm{d}\hat{\mathbf{k}}\,D^{\ell}_{mp}(\phi_{\mathbf{k}},\theta_{\mathbf{k}},0)D^{\ell'}_{m'p}(\phi_{\mathbf{k}},\theta_{\mathbf{k}},0)}_{=\frac{4\pi}{2\ell+1}\delta_{\ell\ell'}\delta_{mm'}} \\
&= \frac{(-\mathrm{i})^{\ell-\ell'}}{\sqrt{(2\ell+1)(2\ell'+1)}}\int \mathrm{d}\ln k\,\mathcal{P}_h(k)\left[\frac{\Theta_\ell^{(p)}(\eta_0,\mathbf{k})}{h^{(p)}(\mathbf{k})}\right]^2 \frac{4\pi}{2\ell+1}\delta_{\ell\ell'}\delta_{mm'} \\
&= \frac{4\pi}{(2\ell+1)^2}\delta_{\ell\ell'}\delta_{mm'}\int \mathrm{d}\ln k\left[\frac{\Theta_\ell^{(p)}(\eta_0,\mathbf{k})}{h^{(p)}(\mathbf{k})}\right]^2 \mathcal{P}_h(k),
\end{aligned}
$$

where formally $\mathrm{d}^3k = k^2\,\mathrm{d}k\,\mathrm{d}\hat{\mathbf{k}}$, and in the third to the fourth lines the Wigner D-matrix orthogonality condition has been used [6].

Comparing with Eqn. (49), we see that the angular power spectrum for temperature anisotropies generated by gravitational waves is simply

$$
C_\ell = \frac{4\pi}{(2\ell+1)^2}\int \mathrm{d}\ln k\left[\frac{\Theta_\ell^{(p)}(\eta_0,\mathbf{k})}{h^{(p)}(\mathbf{k})}\right]^2 \mathcal{P}_h(k). \tag{64}
$$

A crude approximation — To gain an intuitive understanding and make use of C_ℓ, we assume that [6]:

1) the shear in gravitational waves is impulsive at horizon entry;

2) the visibility function is sharply peaked at the time of recombination η_*, so $\tau\big|_{\eta>\eta_*} = 0$;

3) the primordial power spectrum $\mathcal{P}_h(k)$ is scale-invariant.

This means that we can write

$$
\dot{h}^{(\pm 2)}(\eta,\mathbf{k}) \sim -\delta(\eta - k^{-1})h^{(\pm 2)}(\mathbf{k}) \tag{65}
$$

and substitute this into Eqns. (63) and (64)

$$
\begin{aligned}
C_\ell &\sim \frac{4\pi}{(2\ell+1)^2}\mathcal{P}_h\int_{\eta_0^{-1}}^{\eta_*^{-1}} \mathrm{d}\ln k \\
&\qquad \times \left[\frac{2\ell+1}{4}\sqrt{\frac{(\ell+2)!}{(\ell-2)!}}\frac{j_\ell(k\eta_0-1)}{(k\eta_0-1)^2}\right]^2 \\
&= \frac{\pi}{4}\frac{(\ell+2)!}{(\ell-2)!}\mathcal{P}_h\int_{\eta_0^{-1}}^{\eta_*^{-1}} \mathrm{d}\ln k\,\frac{j_\ell^2(k\eta_0-1)}{(k\eta_0-1)^4} \\
&= \frac{\pi}{4}\frac{(\ell+2)!}{(\ell-2)!}\mathcal{P}_h\int_0^{\eta_0/\eta_*-1} \frac{\mathrm{d}x}{1+x}\frac{j_\ell^2(x)}{x^4} \\
&\approx \frac{\pi}{4}\frac{(\ell+2)!}{(\ell-2)!}\mathcal{P}_h\int_0^{\infty} \mathrm{d}x\,\frac{j_\ell^2(x)}{x^5}.
\end{aligned}
$$

To arrive at the last line, we note that for $1 \ll \ell \ll \eta_0/\eta_* \approx 60$, the integral is dominated by $x \approx l$. Finally, using the numerical formula [6]

$$
\int_0^\infty \mathrm{d}x\,\frac{j_\ell^2(x)}{x^5} = \frac{4}{15}\frac{(\ell-1)!}{(\ell+3)!},
$$

we have

$$
C_\ell \sim \frac{\pi}{15}\frac{1}{(\ell-2)(\ell+2)}\mathcal{P}_h. \tag{66}
$$

Because of our approximation, this scale-invariant angular power spectrum is only valid for gravitational waves on scales $\ell \in (1,60)$ which enter the horizon after last-scattering ($\eta_* < k^{-1} < \eta_0$).

III.2 Polarisation from PGWs

III.2.1 Concepts and notions

Stokes parameters — In analogy with electromagnetism where the correlation matrix of the electric fields for a plane wave propagating in direction $\hat{\mathbf{z}}$ are captured by the 4 real parameters I, Q, U and V

$$\begin{pmatrix} \langle E_x E_x^* \rangle & \langle E_x E_y^* \rangle \\ \langle E_y E_x^* \rangle & \langle E_y E_y^* \rangle \end{pmatrix} \equiv \frac{1}{2} \begin{pmatrix} I+Q & U+\mathrm{i}V \\ U-\mathrm{i}V & I-Q \end{pmatrix}, \tag{67}$$

we could also characterise the polarisation of the CMB using these Stokes parameters.[2] The trace is the total intensity I, the difference between intensities in x- and y-directions is Q and U the difference when x, y-axes are rotated by 45°. V describes circular polarisation, which vanishes for Thomson scattering [6].

Spin — Locally the propagation direction $\mathbf{e}$ of the observed photon and its associated spherical polar unit vectors $\hat{\boldsymbol{\theta}}$, $\hat{\boldsymbol{\phi}}$ form a right-handed basis. In the plane spanned by $\hat{\boldsymbol{\theta}}$, $\hat{\boldsymbol{\phi}}$, we define the complex null basis

$$\mathbf{m}_\pm := \hat{\boldsymbol{\theta}} \pm \mathrm{i}\hat{\boldsymbol{\phi}} \tag{68}$$

with respect to which the linear Stokes parameters are determined. Under a left-handed rotation through angle ψ about $\mathbf{e}$,

$$\mathbf{m}_\pm \longrightarrow \mathrm{e}^{\pm \mathrm{i}\psi} \mathbf{m}_\pm;$$

a quantity on the 2-sphere ${}_s\eta$ is said to be spin s if it correspondingly transforms as

$${}_s\eta \longrightarrow \mathrm{e}^{\mathrm{i}s\psi}\, {}_s\eta, \tag{69}$$

e.g. $Q \pm \mathrm{i}U$ has spin ± 2.

Spin-weighted spherical harmonics — The spin-raising and spin-lowering operators $\eth$ and $\bar{\eth}$ act on a spin-s quantity ${}_s\eta$ as

$$\begin{aligned} \eth\, {}_s\eta &= -\sin^s\theta(\partial_\theta + \mathrm{i}\,\mathrm{cosec}\,\theta\partial_\phi)\sin^{-s}\theta\, {}_s\eta, \\ \bar{\eth}\, {}_s\eta &= -\sin^{-s}\theta(\partial_\theta - \mathrm{i}\,\mathrm{cosec}\,\theta\partial_\phi)\sin^{s}\theta\, {}_s\eta. \end{aligned} \tag{70}$$

We can now define the spin-weighted spherical harmonics

$${}_sY_{\ell m} = \sqrt{\frac{(\ell-|s|)!}{(\ell+|s|)!}}\,\eth^s Y_{\ell m} \tag{71}$$

where [7] $\eth^{-|s|} \equiv (-1)^s \bar{\eth}^{|s|}$. Numerous ${}_sY_{\ell m}$ properties, which are useful in subsequent calculations, are listed in Appendix F.

Linear polarisation tensor — In the coordinate basis, we can write the complex null basis vectors $m_\pm$ as

$$m_\pm^a = (\partial_\theta)^a \pm \mathrm{i}\,\mathrm{cosec}\,\theta(\partial_\phi)^a. \tag{72}$$

The linear polarisation tensor can then be expressed as

$$P^{ab} = \frac{1}{4}\Big[(Q+\mathrm{i}U)m_-^a m_-^b + (Q-\mathrm{i}U)m_+^a m_+^b\Big]. \tag{73}$$

This relates to the symmetric traceless part of Eqn. (67): the projection of P_{ab} onto the complex null basis gives

$$Q \pm \mathrm{i}U = m_\pm^a m_\pm^b P_{ab}. \tag{74}$$

E- and B-modes — We can decompose the symmetric traceless linear polarisation tensor as

$$P_{ab} = \nabla_{\langle a}\nabla_{b\rangle}P_E + \varepsilon^c{}_{(a}\nabla_{b)}\nabla_c P_B \tag{75}$$

for some real scalar potentials P_E, P_B. Here ε is the alternating tensor and $\langle\ \rangle$ denotes the symmetric traceless part of a tensor, i.e. $\nabla_{\langle a}\nabla_{b\rangle} = \nabla_{(a}\nabla_{b)} - g_{ab}\nabla^2/2$. Then (see derivations in Appendix G)

$$\begin{aligned} Q + \mathrm{i}U &= \eth\,\eth(P_E + \mathrm{i}P_B), \\ Q - \mathrm{i}U &= \bar{\eth}\,\bar{\eth}(P_E - \mathrm{i}P_B). \end{aligned} \tag{76}$$

As in the case for temperature anisotropies, we may expand in spherical harmonics the fields

$$\begin{aligned} P_E(\mathbf{e}) &= \sum_{\ell,m}\sqrt{\frac{(\ell-2)!}{(\ell+2)!}}E_{\ell m}Y_{\ell m}(\mathbf{e}) \\ P_B(\mathbf{e}) &= \sum_{\ell,m}\sqrt{\frac{(\ell-2)!}{(\ell+2)!}}B_{\ell m}Y_{\ell m}(\mathbf{e}) \end{aligned} \tag{77}$$

so that

$$(Q \pm \mathrm{i}U)(\mathbf{e}) = \sum_{\ell,m}(E_{\ell m} \pm \mathrm{i}B_{\ell m})\,{}_{\pm 2}Y_{\ell m}(\mathbf{e}). \tag{78}$$

These coefficients $E_{\ell m}$ and $B_{\ell m}$ are associated with what are known as E- and B-mode CMB polarisation induced by (primordial) gravitational waves.

III.2.2 The Boltzmann equation for polarisation

Pre-recombination polarisation is negligible since efficient Thomson scattering isotropises CMB radiation.

[2] The average is taken over a time span longer than the wave period but shorter in comparison with amplitude variations. In analogy with Eqn. (51), these parameters are defined for the frequency independent fractional thermodynamic equivalent temperatures [7].

Towards recombination, the mean-free path of photons increases until they can free-stream over an appreciable distance (compared with the wavelength associated with perturbations) between scatterings such that a temperature quadrupole is generated [6]. The linear polarisation observed today is directly related to quadrupole anisotropies at the time of last-scattering [8], and standard results in scattering theory give *the Boltzmann equation for linear polarisation*

$$\frac{\mathrm{d}(Q \pm \mathrm{i}U)(\mathbf{e})}{\mathrm{d}\eta} = \dot{\tau}(Q \pm \mathrm{i}U)(\mathbf{e}) - \frac{3}{5}\dot{\tau} \sum_{|m|\leqslant 2} \left(E_{2m} - \frac{1}{\sqrt{6}}\Theta_{2m} \right) {}_{\pm 2}Y_{2m}(\mathbf{e}). \quad (79)$$

where $\mathrm{d}/\mathrm{d}\eta$ is along the background lightcone [7].

By using the integrating factor $\mathrm{e}^{-\tau}$ again as we did for deriving Eqn. (58), we obtain a line-of-sight integral solution to the polarisation observed today

$$(Q \pm \mathrm{i}U)(\eta_0, \mathbf{x}_0, \mathbf{e}) = -\frac{\sqrt{6}}{10} \sum_{|m|\leqslant 2} \int_0^{\eta_0} \mathrm{d}\eta\, g(\eta) \times \left(\Theta_{2m} - \sqrt{6}E_{2m} \right)(\eta, \mathbf{x}_0 - \chi\mathbf{e})\, {}_{\pm 2}Y_{2m}(\mathbf{e}) \quad (80)$$

where $\chi = \eta_0 - \eta$.

Note that if reionisation is absent, the integral mainly receives contributions from the time of recombination.

III.2.3 Linear polarisation from gravitational waves

We shall now consider the generation of linear polarisation from gravitational waves, and thus restore the polarisation labels (p). If we neglect reionisation and treat last-scattering as instantaneous [6], i.e. $g(\eta) \approx \delta(\eta - \eta_*)$ where we have reused η_* to denote the conformal time at last-scattering, which takes place close to recombination, then the integral solution (80) above becomes

$$(Q \pm \mathrm{i}U)(\eta_0, \mathbf{x}_0, \mathbf{e}) = -\frac{\sqrt{6}}{10} \times \sum_{|m|\leqslant 2} \left(\Theta_{2m} - \sqrt{6}E_{2m} \right)(\eta_*, \mathbf{x}_*)\, {}_{\pm 2}Y_{2m}(\mathbf{e}) \quad (81)$$

where $\mathbf{x}_* = \mathbf{x}_0 - \chi_*\mathbf{e}$ and $\chi_* = \eta_0 - \eta_*$. Now Eqn. (62) says in Fourier space,

$$\Theta^{(p)}_{\ell m}(\eta, \mathbf{k}) = \frac{1}{\sqrt{2}}(-\mathrm{i})^\ell \Theta^{(p)}_\ell(\eta, \mathbf{k}) \times \sqrt{\frac{4\pi}{2\ell+1}} D^\ell_{mp}(\phi_\mathbf{k}, \theta_\mathbf{k}, 0),$$

and similar expressions hold for $E_{\ell m}$ and $B_{\ell m}$. With the substitution of the equation above set to $\ell = 2$, taking the Fourier transform of Eqn. (81) (with respect to $\mathbf{x}_0$) yields the polarisation generated by a single helicity-p state

$$\begin{aligned}(Q \pm \mathrm{i}U)(\eta_0, \mathbf{k}, \mathbf{e}) &= \left(-\frac{\sqrt{6}}{10} \right) \frac{1}{\sqrt{2}}(-\mathrm{i})^2 \sqrt{\frac{4\pi}{5}} \left(\Theta^{(p)}_2 - \sqrt{6}E^{(p)}_2 \right)(\eta_*, \mathbf{k})\, \mathrm{e}^{-\mathrm{i}k\chi_*\hat{\mathbf{k}}\cdot\mathbf{e}} \sum_{|m|\leqslant 2} D^2_{mp}(\phi_\mathbf{k}, \theta_\mathbf{k}, 0)\, {}_{\pm 2}Y_{2m}(\mathbf{e}) \\ &= \frac{1}{10}\sqrt{\frac{12\pi}{5}} \left(\Theta^{(p)}_2 - \sqrt{6}E^{(p)}_2 \right)(\eta_*, \mathbf{k})\, \mathrm{e}^{-\mathrm{i}k\chi_*\hat{\mathbf{k}}\cdot\mathbf{e}} \sum_{|m|\leqslant 2} D^2_{mp}(\phi_\mathbf{k}, \theta_\mathbf{k}, 0)\, {}_{\pm 2}Y_{2m}(\mathbf{e}), \end{aligned} \quad (82)$$

where we have used the translation property of Fourier transform, resulting in the modulation by a phase factor.

To determine the angular power spectra associated with E- and B-modes, we must evaluate the polarisation contribution above from gravitational waves. First taking $\hat{\mathbf{k}} = \hat{\mathbf{z}}$, we obtain the following expression (see calculations in Appendix H)

$$(Q \pm \mathrm{i}U)(\eta_0, k\hat{\mathbf{z}}, \mathbf{e}) \propto -\sqrt{5} \sum_\ell (-\mathrm{i})^\ell \sqrt{2\ell+1} \times {}_{\pm 2}Y_{\ell p}(\mathbf{e}) \left[\epsilon_\ell(k\chi_*) \pm \frac{p}{2}\mathrm{i}\beta_\ell(k\chi_*) \right] \quad (83)$$

where the *projection functions* are

$$\begin{aligned} \epsilon_\ell(x) &:= \frac{1}{4}\left[\frac{\mathrm{d}^2 j_\ell}{\mathrm{d}x^2} + \frac{4}{x}\frac{\mathrm{d}j_\ell}{\mathrm{d}x} + \left(\frac{2}{x^2} - 1 \right) j_\ell \right], \\ \beta_\ell(x) &:= \frac{1}{2}\left(\frac{\mathrm{d}j_\ell}{\mathrm{d}x} + \frac{2}{x} j_\ell \right). \end{aligned} \quad (84)$$

By comparing results Eqns. (83) and (84) with Eqn. (78), we act with $D^\ell_{m\pm 2}(\phi_\mathbf{k}, \theta_\mathbf{k}, 0)$ to find for general direc-

tions $\hat{\mathbf{k}}$

$$\begin{aligned}
&\begin{Bmatrix} E^{(\pm 2)}_{\ell m}(\eta_0,\mathbf{k}) \\ B^{(\pm 2)}_{\ell m}(\eta_0,\mathbf{k}) \end{Bmatrix} \\
&= -\frac{\sqrt{5}}{10}\sqrt{\frac{12\pi}{5}}(-\mathrm{i})^\ell\sqrt{2\ell+1}\left(\Theta_2^{(\pm 2)} - \sqrt{6}E_2^{(\pm 2)}\right)(\eta_*,\mathbf{k}) \\
&\qquad\qquad \times \begin{Bmatrix} \epsilon_\ell(k\chi_*) \\ \pm\beta_\ell(k\chi_*) \end{Bmatrix} D^\ell_{m\pm 2}(\phi_{\mathbf{k}},\theta_{\mathbf{k}},0) \\
&= -\frac{\sqrt{12\pi}}{10}(-\mathrm{i})^\ell\sqrt{2\ell+1}\left(\Theta_2^{(\pm 2)} - \sqrt{6}E_2^{(\pm 2)}\right)(\eta_*,\mathbf{k}) \\
&\qquad\qquad \times \begin{Bmatrix} \epsilon_\ell(k\chi_*) \\ \pm\beta_\ell(k\chi_*) \end{Bmatrix} D^\ell_{m\pm 2}(\phi_{\mathbf{k}},\theta_{\mathbf{k}},0) \quad (85)
\end{aligned}$$

where the pre-factors have been restored.

Now we can write down the E- and B-mode power spectra using the orthogonality condition of Wigner D-matrices, since it is analogous to calculating the temperature anisotropy power spectrum:

$$\begin{aligned}
\begin{Bmatrix} C^E_\ell \\ C^B_\ell \end{Bmatrix} &= \frac{6\pi}{25}\int \mathrm{d}\ln k\, \mathcal{P}_h(k) \\
&\times \left[\frac{\left(\Theta_2^{(p)} - \sqrt{6}E_2^{(p)}\right)(\eta_*,\mathbf{k})}{h^{(p)}(\mathbf{k})}\right]^2 \begin{Bmatrix} \epsilon^2_\ell(k\chi_*) \\ \beta^2_\ell(k\chi_*) \end{Bmatrix} \quad (86)
\end{aligned}$$

where $h^{(p)}(\mathbf{k})$ is primordial, $\left(\Theta_2^{(p)} - \sqrt{6}E_2^{(p)}\right)/h^{(p)}$ is independent of the polarisation state and we have summed over the helicity states $p = \pm 2$.

Tight-coupling and large-angle behaviour — Physically, we expect a temperature quadrupole to build up over a scattering time scale due to the shear of gravitational waves $\Theta(\mathbf{e}) \sim -(l_\mathrm{p}/2)\dot{h}_{ij}e^ie^j$, where l_p is the photon mean-free path close to recombination [7]. A more in-depth treatment using the tight-coupling approximation and polarisation-dependent scattering shows that [6]

$$\left(\Theta_2^{(p)} - \sqrt{6}E_2^{(p)}\right)(\eta,\mathbf{k}) \approx \frac{5}{3\sqrt{3}}l_\mathrm{p}\dot{h}^{(p)}(\eta,\mathbf{k}). \quad (87)$$

Substitution of this into Eqn. (86) gives

$$\begin{aligned}
\begin{Bmatrix} C^E_\ell \\ C^B_\ell \end{Bmatrix} &= \frac{2\pi}{9}l_\mathrm{p}^2\mathcal{P}_h\int \mathrm{d}\ln k \\
&\times \left[\frac{\dot{h}^{(p)}(\eta_*,\mathbf{k})}{h^{(p)}(\mathbf{k})}\right]^2 \begin{Bmatrix} \epsilon^2_\ell(k\chi_*) \\ \beta^2_\ell(k\chi_*) \end{Bmatrix}. \quad (88)
\end{aligned}$$

On scales outside the horizon at matter–radiation equality, the form of the gravitational wave shear in the matter-dominated era is derived in Appendix B

$$\dot{h}^{(p)}(\eta,\mathbf{k}) = -3h^{(p)}(\mathbf{k})\frac{j_2(k\eta)}{\eta}, \quad (89)$$

where $h^{(p)}(\mathbf{k})$ is the primordial value. Thus the integrand here contains the product of factors $j_2^2(k\eta_*)$ and $\epsilon^2_\ell(k\chi_*)$ (or β^2_ℓ). The first factor peaks around $k\eta_* \approx 2$, whereas the second factor peaks around $k\chi_* \approx l$. Hence for large-angle behaviour $l \ll \chi_*/\eta_*$, the integral is dominated by modes with $k\chi_* \gg l$ at the right tails of ϵ^2_ℓ (or β^2_ℓ).

The explicit forms (84) of ϵ_ℓ and β_ℓ and the asymptotic expression for spherical Bessel functions $j_\ell(x) \sim x^{-1}\sin(x - \ell\pi/2)$ give

$$\begin{aligned}
\epsilon_\ell(x) &\sim -\frac{1}{2x}\sin\left(x - \frac{\ell\pi}{2}\right), \\
\beta_\ell(x) &\sim \frac{1}{2x}\cos\left(x - \frac{\ell\pi}{2}\right).
\end{aligned}$$

$\epsilon^2_\ell(x)$ and $\beta^2_\ell(x)$ are rapidly oscillating and thus can be replaced by their averages in the integral, i.e. $\epsilon_\ell(x), \beta_\ell(x) \to 1/8x^2$, so we are left with

$$\begin{aligned}
C^E_\ell, C^B_\ell &\approx \frac{\pi\mathcal{P}_h}{4}\left(\frac{l_\mathrm{p}}{\chi_*}\right)^2\int_0^\infty \frac{\mathrm{d}x}{x^3}j_2^2(x) \\
&\approx \frac{\pi\mathcal{P}_h}{288}\left(\frac{l_\mathrm{p}}{\chi_*}\right)^2.
\end{aligned}$$

We see therefore the E- and B-mode polarisation generated by gravitational waves has roughly equal powers on large scales.

III.2.4 Statistics of the CMB polarisation

Cross-correlation — The angular power spectrum encodes the auto-correlation of an observable obeying rotational invariance, but we can also have cross-correlations between different observables, e.g. the two-point correlation between E- and B-modes

$$\left\langle E_{\ell m}B^*_{\ell' m'}\right\rangle = C^{EB}_\ell\delta_{\ell\ell'}\delta_{mm'}, \quad (90)$$

or between temperature anisotropies and polarisation [9]

$$\begin{aligned}
\left\langle \Theta_{\ell m}E^*_{\ell' m'}\right\rangle &= C^{\Theta E}_\ell\delta_{\ell\ell'}\delta_{mm'}, \\
\left\langle \Theta_{\ell m}B^*_{\ell' m'}\right\rangle &= C^{\Theta B}_\ell\delta_{\ell\ell'}\delta_{mm'}.
\end{aligned} \quad (91)$$

Parity symmetry — A possible further constraint on the polarisation statistics is parity invariance. The E- and

B-modes possess *electric parity* and *magnetic parity* respectively;[3] that is under a parity transformation [7]

$$E_{\ell m} \longrightarrow (-1)^{\ell} E_{\ell m}, \quad B_{\ell m} \longrightarrow (-1)^{\ell+1} B_{\ell m}. \tag{92}$$

Non-violation of statistical isotropy and parity symmetry necessarily implies zero cross-correlation between B and Θ or E.

Cosmic variance — As the confrontation between theory and observations often lies between the predictions for the probability distribution and the measurements of the physical variables, it is impossible to avoid mentioning estimators and statistical variance. In observational cosmology, the *intrinsic* cosmic variance arises as one attempts to estimate ensemble expectations with only one realisation of the universe, which contributes to the overall experimental errors [6].

Given a general zero-mean random field $f(\hat{\mathbf{n}})$ on the 2-sphere, we measure the spherical multipoles $f_{\ell m}$ and construct the *unbiased* estimator

$$\hat{C}_\ell = \frac{1}{2\ell+1} \sum_m f_{\ell m} f^*_{\ell m} \tag{93}$$

for the corresponding true angular power spectrum C_ℓ. This has a variance [6]

$$\operatorname{var} \hat{C}_\ell = \frac{2}{2\ell+1} C_\ell^2 \tag{94}$$

due to the fact that we only have $2\ell+1$ independent modes for any given multipole.

Therefore an estimator for cross-correlation may be, for example [9],

$$\hat{C}_\ell^{EB} = \frac{1}{2\ell+1} \sum_m E_{\ell m} B^*_{\ell m};$$

the cosmic variance for auto-correlations may be, for example,

$$\operatorname{var} \hat{C}_\ell^{E} = \frac{2}{2\ell+1} C_\ell^E C_\ell^E;$$

and for cross-correlations [7],

$$\operatorname{var} \hat{C}_\ell^{\Theta E} = \frac{1}{2\ell+1}\left(C_\ell^{\Theta E} C_\ell^{\Theta E} + C_\ell^{\Theta} C_\ell^{E}\right),$$
$$\operatorname{var} \hat{C}_\ell^{\Theta B} = \frac{1}{2\ell+1}\left(C_\ell^{\Theta B} C_\ell^{\Theta B} + C_\ell^{\Theta} C_\ell^{B}\right).$$

[3] This follows from that under a parity transformation, $\mathbf{e} \to -\mathbf{e}$, but $\hat{\boldsymbol{\theta}}(-\mathbf{e}) = \hat{\boldsymbol{\theta}}(\mathbf{e})$ and $\hat{\phi}(-\mathbf{e}) = -\hat{\phi}(\mathbf{e})$ so $(Q \pm \mathrm{i}U)(\mathbf{e}) \to (Q \mp \mathrm{i}U)(-\mathbf{e})$.

IV *B*-Mode Polarisation: A Promising Route for Detecting PGWs?

The measurements of CMB polarisation will soon be of critical importance in modern cosmology: the polarisation signal and the cross-correlations provide consistency checks for standard cosmology, and complement the cosmological information encoded in temperature anisotropies, which are ultimately bound by cosmic variance; the definitive detection of B-mode would indicate non-scalar perturbations, distinguishing different types of primordial fluctuations and imposing significant constraints on cosmological models [1, 6]. In particular, for our purposes, the measurements of B-mode polarisation offers a promising route for detecting primordial gravitational waves.

IV.1 Cosmological sources of *B*-mode polarisation

(Primordial) perturbations in background spacetime may be decomposed into scalar, vector and tensor types, which crucially decouple at linear order [1]. The E- and B-mode split of CMB polarisation has implications on what type of fluctuations may be present during the inflationary period [9, 10]:

1) scalar perturbations create only E- not B-mode polarisation;
2) vector perturbations create mostly B-mode polarisation;
3) tensor perturbations create both E- and B-mode polarisation.

We have proved the last claim in §§ III.2.3, and as for the first claim, one can intuitively see that scalar perturbations do not possess any handedness so they cannot create any B-modes which are associated with the "curl" patterns in CMB temperature maps, but vector and tensor perturbations can [9].

Although we can show this directly just as in §§ III.2.3 but for scalar perturbations, we will instead argue from the Boltzmann equation (79) for linear polarisation by showing that (see details in Appendix I)

$$\dot{E}_\ell + k\left[\sqrt{\frac{(\ell+1)^2-4}{2\ell+3}} E_{\ell+1} - \sqrt{\frac{\ell^2-4}{2\ell-1}} E_{\ell-1}\right] = \dot{\tau}\left[E_\ell - \frac{3}{5}\delta_{\ell 2}\left(E_2 - \frac{1}{\sqrt{6}}\Theta_2\right)\right], \tag{95}$$

$$\dot{B}_\ell + k\left[\sqrt{\frac{(\ell+1)^2-4}{2\ell+3}}B_{\ell+1} - \sqrt{\frac{\ell^2-4}{2\ell-1}}B_{\ell-1}\right] = \dot{\tau}B_\ell. \quad (96)$$

We see that the B-mode equation (96) does not have a source term from temperature quadrupoles, so scalar perturbations do not produce B-mode polarisation.

For B-mode polarisation to truly vindicate the existence of primordial gravitational waves, we must consider other cosmological sources of B-modes. These include: 1) topological defects; 2) global phase transition; 3) primordial inhomogeneous magnetic fields; 4) gravitational lensing.

Topological defects — We have remarked in § II.3 that primordial vector modes are diluted away with expansion. However, topological defects such as cosmic strings, which are often found in grand unification models, actively and efficiently produce vector perturbations which in turn create B-mode polarisation [1]. Nonetheless, the presence of topological defects alone poorly accounts for the polarisation signals seen in the data of the BICEP2 Collaboration[4] [11]. The peaks produced by cosmic strings in the polarisation spectrum, if they are formed, are at high $\ell \sim 600$–1000 (generated at last-scattering) and at low $\ell \sim 10$ (generated at reionisation).

Global phase transitions — It has been shown on dimensional grounds and by simulations that the symmetry-breaking phase transition of a self-ordering scalar field could causally produce a scale-invariant spectrum of gravitational waves [12]. However, similar to topological defects, global phase transitions of self-order scalar field do not reproduce the BICEP2 data [13].

The key physical point is that in these two alternative cosmological models of B-mode polarisation, the causally-produced fluctuations are on sub-horizon scales; only the inflationary model alters the causal structure of the very early universe and accounts for correlations on super-horizon scales [13, 14]. The distinctive signature of an anti-correlation between CMB temperature and polarisation, imprinted by adiabatic fluctuations at recombination and seen on large scales $\ell \sim 50$–150 in WMAP[5] data, is convincing evidence for the inflation theory [7].

[4] Acronym for Background Imaging of Cosmic Extragalactic Polarisation.

[5] Acronym for the Wilkinson Microwave Anisotropy Probe.

Primordial inhomogeneous magnetic fields — In the early universe, magnetic anisotropic stress can generate both vorticity and gravitational waves, and leave signatures in the CMB temperature anisotropy and polarisation (including B-modes). However, these primordial fields are not well-motivated by theoretical models, which predict either very small field amplitudes or a blue tilt in n_s. Furthermore, they can be distinguished from primordial gravitational waves by their non-Gaussianity, or detection of the Faraday effect [15] (interaction between light and magnetic fields in a medium).

Gravitational lensing — This deforms the polarisation pattern on the sky by shifting the positions of photons relative to the last-scattering surface. Some E-mode polarisation is consequently converted to B-modes, as the geometric relation between polarisation direction and angular variations in the E-mode amplitude is not preserved [7]. More in-depth investigations of lensing effects and careful de-lensing work are needed to remove its contamination of the primordial B-mode signal (see further discussions in § VI.1).

IV.2 Statistical aspects of B-mode polarisation

The observational importance of CMB polarisation also stems from the exhaustion of information that could ever be extracted from CMB temperature anisotropies (and E-mode polarisation). Soon the cosmic variance intrinsic to the latter would fundamentally limit our ability to achieve much greater accuracies [16]; in particular, we see that the weighting factor $(2\ell+1)^{-1}$ in Eqn. (94) attributes greater variances at lower ℓ, i.e. on large scales of our interests where gravitational waves (GWs) contribute significantly to anisotropies[6].

To demonstrate this point, we turn to the tensor-to-scalar ratio r introduced in §§ II.3.1 as an example: imagine that r is the only unknown variable and our measurements of large-scale temperature anisotropies are noise-free. We saw in §§ III.1.4 that $C_\ell \sim \mathcal{P}_h \sim A_t$ for gravitational waves, and similarly for curvature perturbations $C_\ell \sim A_s$, so we can estimate r as the excess power over C_ℓ

$$\hat{r}_\ell = \frac{\hat{C}_\ell - C_\ell}{C_\ell^{\rm GW}(r=1)} \quad (97)$$

using a set of angular power spectrum estimators [6]

[6] In Appendix B, we show that as the universe expands gravitational waves are damped by the scale factor within the Hubble horizon.

$\hat{C}_\ell$ given in §§ III.2.4. Here C_ℓ is the true angular power spectrum from curvature perturbations, and $C_\ell^{\rm GW}(r = 1)$ is the true angular power spectrum from GWs if r were equal to 1.

Amongst all weighted averages, the inverse-variance weighting gives the least variance, so one can make a prediction on the error $\sigma(r)$ in the null hypothesis $H_0 : r = 0$,

$$\frac{1}{\sigma^2(r)} = \sum_\ell \frac{2\ell+1}{2}\left[\frac{C_\ell^{\rm GW}(r=1)}{C_\ell}\right]^2. \tag{98}$$

Approximating $C_\ell^{\rm GW}(r = 1)/C_\ell \approx 0.4$ as constant for $\ell < 60$, we obtain a rough estimate

$$\frac{1}{\sigma^2(r)} \approx \frac{0.4^2}{2} \times (60+1)^2 \quad \Longrightarrow \quad \sigma(r) \approx 0.06.$$

Using the actual spectra observed gives $\sigma(r) = 0.08$ which is not far from our rough estimate [6]. The latest Planck data puts an upper bound $r < 0.10 - 0.11$ at 95% confidence level (CL) [17], consistent with $r = 0$. We thus see that the scope of detecting PGWs within temperature anisotropies alone is slim.

On the other hand, the CMB B-mode polarisation may circumvent this problem: it receives no scalar contributions, and is unlike the temperature anisotropies and E-mode polarisation to which the gravitation wave contribution is sub-dominant [6]. The peak location and the peak height of the polarisation power spectrum are sensitive to the epoch of last-scattering when perturbation theory is still in the linear regime: they depend, respectively, on the horizon size at last-scattering and its duration; this signature is not limited by cosmic variance until late reionisation [8]. In contrast, temperature fluctuations can alter between last-scattering and today, e.g. through the integrated Sachs–Wolfe effect of an evolving gravitational potential. Therefore B-mode polarisation complements information extracted from temperature anisotropies and already-detected E-mode polarisation [18], and offers a promising route for primordial gravitational wave detection.

V A "Smoking Gun": Physical Significance of PGW Discovery

Having discussed the causal mechanism, the cosmological imprints and the practical detection of primordial gravitational waves, we now turn to the significance of a PGW discovery. As we mentioned earlier in this paper, the theory of inflation solves a number of puzzles in standard Big Bang cosmology; quantum fluctuations in the very early universe are amplified and subsequently frozen in on super-horizon scales, seeding large-scale structure formation. Detecting PGWs provides strong evidence for the existence of inflation, and in addition it will reveal to us

- the energy scale of inflation and thus that of the very early universe;
- the amplitude of the inflaton field excursion which constrains models of inflation;
- any violation of the various consistency conditions for testing inflation models;
- clues about modified gravity and particle physics beyond the Standard Model.

The last point is anticipated as the validation of inflation theory inevitably involves the testing of all fundamental theories upon which it is built. The links between primordial gravitational waves and modified gravity and effective field theory are explored in some recent literature [19]. We shall here consider the other points in turn.

V.1 Alternatives to inflation

To validate the inflation theory we must consider competing cosmological models, which chiefly include [1]: 1) ekpyrotic cosmology; 2) string gas cosmology; 3) pre-Big Bang cosmology.

Ekpyrotic cosmology — In this model, the universe starts from a cold beginning, followed by slow contraction and then a bounce returning to the standard FLRW cosmology. Its cyclic extension presents a scenario where the ekpyrotic phase recurs indefinitely. It has been shown that in this model, not only quantum fluctuations but inhomogeneities are also exponentially amplified without fine-tuning [20]; during the bouncing phase, the null energy condition is violated—a sign usually associated with instabilities [1]; furthermore, taking gravitational back-reaction into account, the curvature spectrum is strongly scale-dependent [21]. In the new ekpyrotic models, some of these issues are resolved; however, a substantial amount of non-Gaussianity is now predicted [22] and more importantly, the absence of detectable levels of PGWs makes it very distinguishable from inflation.

String gas cosmology — This model assumes a hot Big Bang start of the universe with energies at the string scale and with compact dimensions. The dynamics

of interacting strings means three spatial dimensions are expected to de-compactify but this requires fine-tuning. Also, a smooth transition from the string gas phase to the standard radiation phase violates the null energy condition, believed to be important in ultraviolet-complete (UV-complete) theories, or the scale-inversion symmetry, believed to be fundamental to string theory; in addition, the production of a nearly scale-invariant power spectrum requires a blue-tilted scalar spectral index [1, 23, 24].

Pre-Big Bang cosmology — Motivated by string gas cosmology, this scenario describes a cold, empty, flat initial state of the universe. Dilatons drive a period of "super-inflation" until the string scale is reached, after which the radiation-dominated era initiates [1, 25]. However, the issue of string phase exit to the radiation phase is poorly understood and some literature claims that the horizon, flatness and isotropy problems in standard cosmology are not explained [26].

To summarise, the key obstacles of current alternative theories to competing with inflation include: 1) failure of a smooth transition to the standard Big Bang evolution; 2) absence of a significant amplitude of primordial gravitational waves. The latter means primordial gravitational waves, and thus B-mode polarisation, are a "smoking gun" of inflation [1].

V.2 Energy scale and the inflaton field excursion

Energy scale of the early universe — Recall that for slow-roll inflation, $\dot{\phi}^2 \ll V$ so Eqns. (1), (3), (39) and (42) together lead to a relation between the energy scale of inflation $V^{1/4}$ and the tensor-to-scalar ration r,

$$V^{1/4} \approx \left(\frac{3\pi^2}{2} r \mathcal{P}_s\right)^{1/4} M_{\rm Pl}. \tag{99}$$

For fiducial values at $r_\star = 0.01$, $k_\star = 0.05\,\mathrm{Mpc}^{-1}$ and $\ln\left(10^{10} A_s\right) = 3.089$ (the value given in [17]), we have calculated that $V_\star^{1/4} \approx 1.03 \times 10^{16}\,\mathrm{GeV}$ using $M_{\rm Pl} = 2.43 \times 10^{18}\,\mathrm{GeV}$, i.e.

$$V^{1/4} = \left(\frac{r}{0.01}\right)^{1/4} 1.06 \times 10^{16}\,\mathrm{GeV}.$$

We see that the energy scale during inflation reaches that of *Grand Unification theories*, just a few orders of magnitude below the Planck scale. It is difficult to overstate the huge implications this has for high-energy particle physics. To date the only hints about physics at such enormous energies are the apparent unification of gauge couplings and the lower bounds on the proton lifetime—such energy scales are forever beyond the reach of human-made ground particle colliders [7]; in comparison, the Large Hadron Collider currently operates at up to 13 TeV [27], lower by $\mathcal{O}\left(10^{13}\right)$.

Lyth bound — We can relate the inflaton field excursion $\Delta\phi$ to the tensor-to-scalar ratio r. Recall in §§ II.3.1 we have derived that $r = 16\epsilon \equiv \left(8/M_{\rm Pl}^2\right)\left(\dot{\phi}/H\right)^2$, which can be written using the number of e-folds $\mathrm{d}N = H\,\mathrm{d}t$ as

$$\frac{r}{8} = \left(\frac{1}{M_{\rm Pl}} \frac{\mathrm{d}\phi}{\mathrm{d}N}\right)^2.$$

Integration gives

$$\frac{\Delta\phi}{M_{\rm Pl}} = \int_0^{N_\star} \mathrm{d}N \sqrt{\frac{r(N)}{8}} \equiv N_{\rm eff} \sqrt{\frac{r_\star}{8}} \tag{100}$$

where $N_\star$ is the number of e-folds between the end of inflation and the horizon exit of the CMB pivot scale, and the *effective number of e-folds*

$$N_{\rm eff} := \int_0^{N_\star} \mathrm{d}N \sqrt{\frac{r(N)}{r_\star}} \tag{101}$$

is model-*dependent* as r evolves [19]. In slow-roll inflation, we can treat ϵ as approximately constant so r also is, giving a lower bound on the inflaton field excursion

$$\frac{\Delta\phi}{M_{\rm Pl}} \gtrsim \sqrt{\frac{r_\star}{8}} N_\star \approx \frac{N_\star}{60} \sqrt{\frac{r_\star}{0.002}}. \tag{102}$$

Hence we see that if at least 60 e-folds are required to solve the flatness and the horizon problems [1], emission of a substantial amount of gravitational waves would mean a super-Planckian field excursion. (A more conservative bound of $N_{\rm eff} = 30$ gives instead $\Delta\phi/M_{\rm Pl} \gtrsim 1.06\sqrt{r_\star/0.01}$, but the conclusion is unaltered.)

Super-Planckian field variation has consequences for inflation model-building. For instance, in the context of supergravity, one may expect the inflaton potential to have an infinite power series, say

$$V = V_0 + \frac{m^2}{2}\phi^2 + \lambda_4\phi^4 + \frac{\lambda_6}{M_{\rm Pl}^2}\phi^6 + \frac{\lambda_8}{M_{\rm Pl}^4}\phi^8 + \cdots.$$

Standard field theories would truncate such series after the first few terms, as is the case in the Standard Model, its minimal supersymmetric extensions and many others [28]. However, for more generic field theories, the coupling coefficients λ arising from integrated-out fields at higher energies may be large, e.g. at

$\mathcal{O}(1)$, in which case the series diverges. A detectable r could place us in an uncharted territory of high-energy physics, propelling advances in beyond-the-Standard-Model UV-complete theories.

V.3 Constraining models of inflation

Broadly speaking, inflation models are classified as: 1) *single-field*, of which single-field slow-roll inflation is a simple case, but including some apparently multi–field models such as hybrid inflation; or 2) *multi-field*, where more than one scalar field is invoked [1].

Generic single-field inflation — Single-field inflation may be *large* or *small* according to the inflaton field excursion, and blue ($n_s > 1$) or red ($n_s < 1$) depending on the *tilt* n_s. Non-canonical kinetic effects may appear in general single-field models given by an action of the form ($M_{\rm Pl} = 1$ here)

$$S = \frac{1}{2}\int \mathrm{d}^4x\,\sqrt{-g}\left[R + 2P(X,\phi)\right] \tag{103}$$

where $X \equiv -g^{\mu\nu}\partial_\mu\phi\partial_\nu\phi/2$, P is the pressure of the scalar fluid and $\rho = 2XP_{,X} - P$ its energy density. For instance, slow-roll inflation has $P(X,\phi) = X - V(\phi)$. These models are characterised by a *speed of sound*

$$c_s := \sqrt{\frac{P_{,X}}{\rho_{,X}}} \tag{104}$$

where $c_s = 1$ for a canonical kinetic term, and $c_s \ll 1$ signals a significant departure from that. In addition, a time-varying speed of sound $c_s(t)$ would alter the prediction for the scalar spectral index as $n_s = -2\epsilon - \eta - s$, where

$$s := \frac{\dot{c}_s}{Hc_s} \tag{105}$$

measures its time-dependence [1].

Multi-field inflation — Multi-field models produce novel features such as large non-Gaussianities with different shapes and amplitudes, and isocurvature perturbations which could leave imprints on CMB anisotropies. However, the extension to ordinary single-field models to include more scalar degrees of freedom also diminishes the predictive power of inflation. Diagnostics beyond the B-mode polarisation may be needed for such models [1].

V.3.1 Model features

Shape of the inflation potential — For single-field slow-roll inflation, we merely say the inflaton potential V remains "flat", i.e. $\epsilon_V \ll 1$ and $\left|\eta_V\right| \ll 1$. In addition to ϵ_V and η_V, the family of potential slow-roll parameters include [17] [cf. Eqn. (8)]

$$\xi_V := M_{\rm Pl}^2\left|\frac{V_{,\phi}V_{,\phi\phi\phi}}{V^2}\right|^{1/2} \quad \text{etc.} \tag{106}$$

which encode derivatives of the inflaton potential at increasing orders, so they control the *shape* of the potential $V(\phi)$. Often in literature (e.g. [1, 7]) the *Hubble slow-roll parameters* defined analogously to the above are adopted, with the potential variable $V(\phi)$ replaced by the Hubble parameter $H(\phi)$.

Deviation from scale-invariance — A perfectly scale-invariant spectrum, i.e. the Harrison–Zel'dovich–Peebles spectrum, has $n_s = 1$. Deviations from scale-invariance may be captured by the scalar spectral index and its *running*

$$\alpha_s := \frac{\mathrm{d}n_s}{\mathrm{d}\ln k}, \tag{107}$$

which parametrise the scalar power spectrum as [cf. Eqn. (28)]

$$\mathcal{P}_s = A_s\left(\frac{k}{k_\star}\right)^{n_s - 1 + \frac{1}{2}\alpha_s \ln\left(\frac{k}{k_\star}\right)}. \tag{108}$$

α_s may be small even for strong scale-dependence as it only arises at second order in slow-roll. A significant value of α_s would mean that the third potential slow-roll parameter ξ_V plays an important role in inflationary dynamics [1, 7].

V.3.2 Significance of the tensor power spectrum

To link the model features above to the detection of PGWs, we observe that the spectral indices are related to the potential slow-roll parameters (in the case of canonical single-field inflation $P = X - V$) by

$$n_s - 1 = 2\eta_V - 6\epsilon_V,$$
$$n_t = -2\epsilon_V$$

at first order. The second equation is Eqn. (43), and the first comes from Eqns. (8) and (26)

$$\begin{aligned} n_s - 1 &= 2\frac{\mathrm{d}\ln H}{\mathrm{d}\ln k} - \frac{\mathrm{d}\ln\epsilon}{\mathrm{d}\ln k} \\ &\approx \frac{2}{H}\frac{\mathrm{d}\ln H}{\mathrm{d}t} - \frac{1}{H}\frac{\mathrm{d}\ln\epsilon}{\mathrm{d}\ln t} \\ &= -2\epsilon - \eta \\ &\approx 2\eta_V - 6\epsilon_V \end{aligned}$$

where we have replaced $\mathrm{d}\ln k = (1-\epsilon)H\,\mathrm{d}t \approx H\,\mathrm{d}t$ at horizon crossing $k = aH$. The runnings α_s and α_t (defined analogously for tensor perturbations) can also be linked to potential slow-roll parameters, so the measurements of r, spectral indices n_s, n_t and runnings α_s, α_t can break the degeneracy in (potential) slow-roll parameters and control the shape of the inflaton potential, thus constraining inflationary models.

Consistency conditions — The measurements of PGW signals can be used to test consistency of different inflation models (see Tab. 1), and therefore filter out single-field inflation through the sound speed, and on multi-field inflation through $\cos\Delta$, which is the directly measurable correlation between adiabatic and isocurvature perturbations for two-field inflation; or more generally through $\sin^2\Delta$, which parametrises the ratio between the adiabatic power spectrum at horizon exit during inflation and the observed power spectrum [1].

Table 1. Consistency conditions for inflation models.

model	consistency conditions
single-field slow-roll	$r = -8n_\mathrm{t}$
generic single-field	$r = -8n_\mathrm{t}c_\mathrm{s}$
multi-field	$r = -8n_\mathrm{t}\sin^2\Delta$

Symmetries in fundamental physics — Sensitivity of inflation to the UV-completion of gravity is a crux in its model-building, but also creates excitement over experimental probes of fundamental physics as the very early universe is the ultimate laboratory for high energy phenomena. Many inflationary models are motivated by string theory, which is by far the best-studied theory of quantum gravity, and supersymmetry is a fundamental spacetime symmetry of that (and others) [1].

Controlling the shape of the inflaton potential over super-Planckian ranges requires an *approximate shift-symmetry* $\phi \to \phi + \text{const.}$ in the ultraviolet limit of the underlying particle theory for inflation. The construction of controlled large-field inflation models with approximate shift symmetries in string theory has been realised recently. Therefore, the inflaton field excursion as inferred from PGW signals could probe the symmetries in fundamental physics, and serve as a selection principle in string-theoretical inflation models [1, 7].

VI Future Experiments: Challenges and Prospects

70 years ago the cosmic microwave background was predicted by Alpher and Hermann; 53 years ago the CMB was "accidentally" discovered by Penzias and Wilson; 25 years ago the CMB anisotropy was first observed by the COBE DMR[7]. What marked the gaps of many years in between was not our ignorance of the signatures encoded in the CMB, but the lack of necessary technology to make precise measurements [16].

Now that has all changed within the last decade or so: observational cosmology has benefited from leaps in precision technology, and many may refer to the present time as the "golden age of cosmology" in implicit parallelism with the golden age of exploration, when new continents were discovered and mapped out [1].

Bounds from current CMB observations — Various cosmological parameters related to inflation [17] have been measured, including but not limited to:

1) a red tilt of $n_\mathrm{s} = 0.9645$–0.9677 at 68% CL depending on the types of data included. The scale-invariant Harrison–Zel'dovich–Peebles spectrum is 5.6σ away;
2) a value of running for scalar perturbations consistent with zero, $\alpha_\mathrm{s} = -0.0033 \pm 0.0074$, with the Planck 2015 full mission temperature data, high-ℓ polarisation and lensing ;
3) an upper bound at 95% CL for the tensor-to-scalar ratio $r_{0.002} < 0.10$–0.11, or $r_{0.002} < 0.18$ assuming nonzero α_s and α_t. The subscript denotes the pivot scale $k_\star$ in units of Mpc^{-1}.

Therefore our current observations disfavour models with a blue tilt, e.g. hybrid inflation, and suggests a negative curvature of the potential $V_{,\phi\phi} < 0$. Models predicting large tensor amplitudes are also virtually ruled out, e.g. the cubic and quartic power law potentials [7]. For the testing of select inflationary models and the reconstruction of a smooth inflaton potential, see [17].

Graphic presentation of current CMB observations — Constraints on the tensor-to-scalar ratio $r_{0.002}$ in the ΛCDM model with B-mode polarisation results

[7] Acronyms for the Cosmic Background Explorer and Differential Microwave Radiometers.

added to existing Planck 2015 results from the BICEP2/Keck Array+Planck default configuration are shown in Fig. 1 (see [29]). The Planck 2015 results have confirmed measurements of temperature anisotropies and E-mode polarisation. The (re-defined) angular power spectra C_ℓ^{EE} and

$$\mathcal{D}_\ell^{TT} := \frac{\ell(\ell+1)}{2\pi} C_\ell^{TT}, \quad \mathcal{D}_\ell^{TE} := \frac{\ell(\ell+1)}{2\pi} C_\ell^{TE}$$

are shown in Fig. 2 (see [30]). A full-sky map of CMB polarisation filtered at around 5° is shown in Fig. 3 (see [31]).

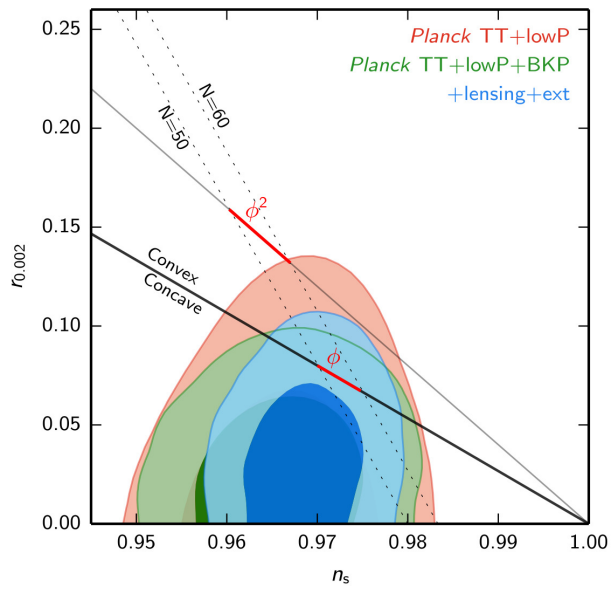

Figure 1. Constraints (68% and 95% CL) on the tensor-to-scalar ratio $r_{0.002}$ in the ΛCDM model with B-mode polarisation results added to existing Planck data from the BICEP2/Keck Array+Planck (BKP) default likelihood configuration. Zero running and consistency relations are assumed. Solid lines show the approximate n_s-r relation for quadratic and linear potentials, to first order in slow roll; the latter separates concave and convex potentials. Dotted lines show loci of approximately constant numbers of e-folds N (from the horizon exit to the end of inflation) for power-law single-field inflation. Credit © ESA/Planck Collaboration.

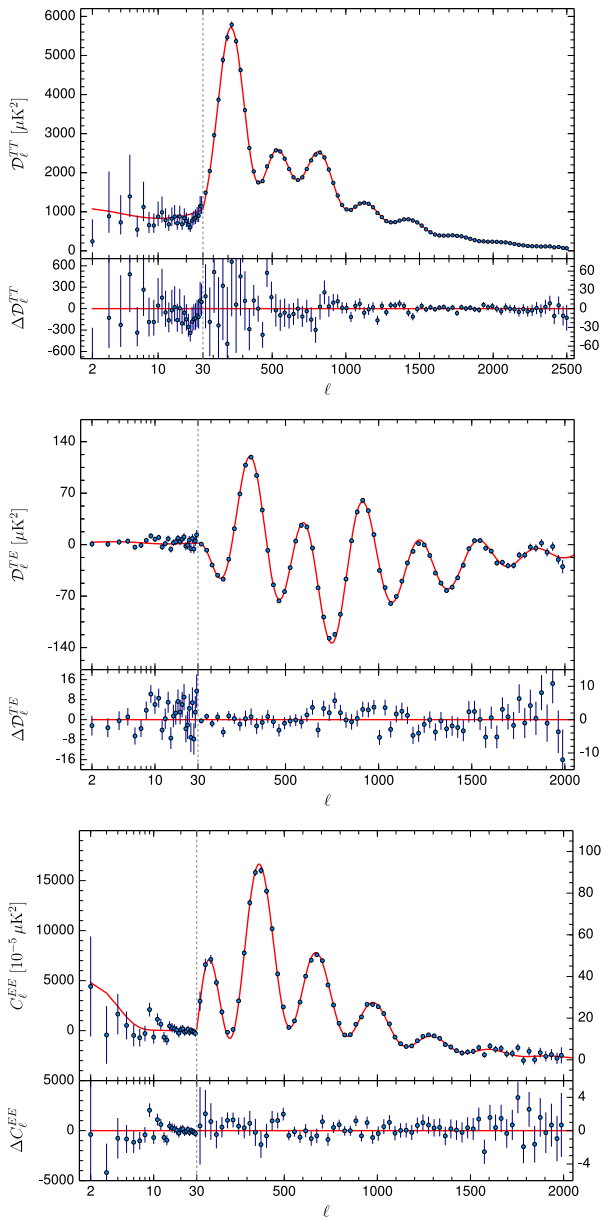

Figure 2. Planck 2015 CMB spectra with the base ΛCDM model fit to full temperature-only and low-ℓ polarisation data. The upper panels show the spectra and the lower panels the residuals. The horizontal scale changes from logarithmic to linear at the "hybridisation" scale $\ell = 29$. Also note the change in vertical scales in lower panels on either side of $\ell = 29$. Credit © ESA/Planck Collaboration.

As it currently stands, the observations of r are not significant enough for the null hypothesis $H_0 : r = 0$ to be rejected. The constraints placed by CMB temperature data on the tensor perturbation amplitude, although improved by the inclusion of Type IA supernova luminosities and baryon acoustic oscillations (BAO)[8] [7], are close to the cosmic variance limit.

Since B-mode polarisation, as we have explained earlier, is a powerful route for vindicating gravitational waves and thus inflation, experimental efforts directed at detecting B-mode signals more sensitively have been driving more stringent constraints on tensor perturbations recently. We shall now present an overview of the experimental challenges and prospects lying ahead in detecting PGWs.

[8] Through more precise values of the matter density and n_s.

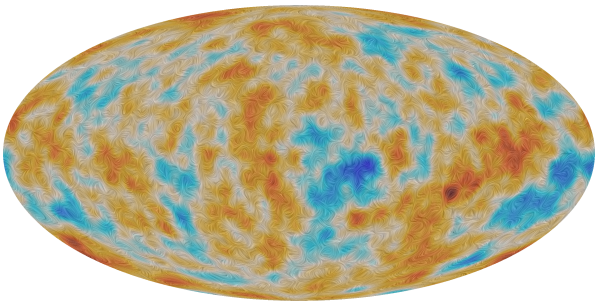

Figure 3. Planck 2015 CMB polarisation filtered at around 5°. Credit © ESA/Planck Collaboration.

VI.1 Challenges in detecting PGWs

The main challenge in detecting PGWs is that the primordial B-mode polarisation signal is faint. The CMB polarisation anisotropy is only a few percent of the temperature anisotropy in the standard thermal history; and B-mode polarisation is at least an order of magnitude lower than the E-mode polarisation [4]. What complicates the picture are reionisation, (weak) gravitational lensing and foreground contamination such as polarised galactic emission (in particular thermal dust emission).

Reionisation — When intergalactic medium begins to reionise, the emitted free electrons re-scatter CMB photons so polarisation signals from last-scattering are suppressed but there is instead a slight increase in polarisation power on large angular scales.[9] This effect controlled by the epoch of reionisation is small and can be analysed by determining the corresponding optical depth $\tau_{\text{reion.}}$ [7].

Gravitational lensing[10] — We have mentioned gravitational lensing as a cosmological source of B-mode polarisation in § IV.1. As polarisation receives contributions from gradients of the baryon velocity but temperature fluctuations from both velocity and density of the photon-baryon plasma which are out of phase, acoustic oscillations are narrower for polarisation spectra than for the temperature anisotropy, and therefore gravitational lensing effects are more significant for the former.

A careful analysis reveals that the converted, extrinsic B-mode from intrinsic E-mode is small in generic models with a peak ($\sim 10\%$ relative change to the undistorted spectra) at angular scales around $\ell \sim 1000$. Recently gravitational lensing in B-mode polarisation has been detected by multiple experiments, in particular in the range $30 < \ell < 150$ which includes the recombination peak [33, 34]. Therefore contamination from lensing could be especially significant for small $r \lesssim 0.01$, and accurate de-lensing work is needed for very high sensitivity measurements in the future.

Instrumentation and astrophysical foregrounds — Current and future CMB experiments should reach a sensitive level that gravitational lensing noise is comparable to instrumental noise, but efforts for improving sensitivity is only sensible if foreground contamination can be removed coherently [7]. The main *astrophysical* foregrounds include the following [8]

1) free-free: although intrinsically unpolarised, free-free emission from ionised hydrogen clouds can be partially polarised due to Thomson scattering. The effect is small and does not dominate at any frequencies;
2) dust: this may be the dominant foreground at high frequencies. Interstellar dust causes microwave thermal emission, which generates E, B-mode polarisation if galactic magnetic fields are present [19]. Recently, the much-reported detection of B-mode polarisation from BICEP2/Keck Array was due to bright dust emission at 353 GHz [35];
3) point sources: these are likely to be negligible except possibly for satellite missions;
4) synchrotron: this is a major concern at low frequencies as it is highly polarised.

There is some scope in exploiting the E, B-mode polarisation nature of foregrounds for their removal, but the technique may be compromised if the foreground produce the two modes unequally. However, multi-frequency coverage in CMB measurements may be able to remove these polarised foregrounds [8].

Looking ahead, the power of any future experiment endeavouring to detect PGWs lies upon three crucial elements [36]: 1) instrumental sensitivity; 2) foreground removal; 3) size of the survey (e.g. angular range of view, number of detectors).

VI.2 Future prospects and concluding remarks

Although the primordial B-mode polarisation signals are weak, there are no fundamental technological or cosmological barriers to achieving great levels sensitivities. The Planck mission has already obtained a

[9] Reionisation also screens temperature anisotropies—uniform screening is important on virtually all scales.

[10] The following discussions on gravitational lensing effects are mostly based on [32].

sensitivity level of $r \sim 0.1$ (not for B-modes though). Next generation of ground-based and balloon experiments surveying smaller regions of the sky with known low-foreground contamination may achieve $r \sim 0.01$, and a dedicated polarisation satellite surveying the full sky, such as CMBPol, may bring this down to $r \sim 0.001$. Levels of such sensitivity would mark a qualitative shift in our capability to test the inflation theory [7, 37].

Satellite missions — Forecasts for a speculative future satellite mission using the Fisher methodology have been made in a concept study, where the theoretical angular power spectra are split into a primordial contribution, a residual foreground contribution and an instrumental noise contribution. For a fiducial model with $r = 0.01$ without foreground contamination, the forecast errors are $\Delta r = 5.4 \times 10^{-4}$ and $\Delta n_t = 0.076$ for a low-cost mission aimed at detecting B-mode polarisation on scales above about 2°. A graphic representation of the forecast constraints in the n_s-r plane with a pessimistic foreground assumption (contamination with residual amplitude 10% in C_ℓ) is shown in Fig. 4. More forecast details can be found in the concept study for the CMBPol mission [1].

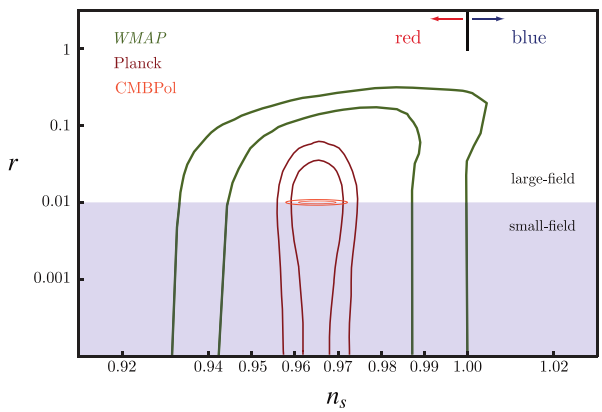

Figure 4. Forecasts of future constraints in the n_s-r plane for a low-cost mission with pessimistic foreground. The contours shown are for 68.3% (1σ) and 95.4% (2σ) CL. Results for WMAP (5-year analysis), Planck and CMBPol are compared (coloured). Large-field and small-field regimes are distinguished at $r = 0.01$. Credit © CMBPol Study Team.

Direct detection[11] — The CMB has provided a powerful window into the very early universe, yet it alone is still not sufficient. One obstacle arises from the tensor spectral index n_t, which is cosmic-variance limited (e.g. it receives residual signals from gravitational lensing); its determination also requires a measurement of the GW amplitudes on different scales. Currently, a value of n_t determined from a full-sky polarisation map, when extrapolated to much smaller wavelengths, has a significant error. Thus to provide even stronger constraints on tensor modes, one must look for other observational channels such as direct detection, e.g. small scale measurements could be performed in laser interferometer experiments. Information from direct detection and from B-mode polarisation can complement each other.

There have already been proposals and concept studies of space-based interferometers such as the Laser Interferometer Space Antenna (LISA) and the Big Bang Observer (BBO). Although the tensor energy density could be very low, BBO may still be able detect its signal at certain frequencies with a high significance level. To separate stochastic PGWs from other cosmological contributions such as global phase transitions, these sources must either be precisely modelled, or experiments with even greater sensitivity (e.g. Ultimate DECIGO[12]) are called for; similarly, astrophysical foregrounds would also need to be better studied and their contamination must be carefully removed.

Cosmic inflation was hypothesised to solve a series of puzzles in standard Big Bang cosmology, but it also provides the causal mechanism for large structure formation. The same mechanism generates a background of stochastic gravitational waves with a nearly scale-invariant spectrum, which leave relatively clean imprints in CMB observables when cosmological perturbations were still in the linear regime.

As it currently stands, the inflation paradigm is still incomplete without a definitive proof of its existence. However, the arrival of precision cosmology has enhanced detection sensitivity to B-mode polarisation by many orders of magnitude; provided we can utilise CMB probes with direct detection and remove foreground contamination with in-depth study of galactic emissions, there is a hopeful prospect that we may observe primordial gravitational waves in the foreseeable future. The confirmed observation would not only vindicate the inflation theory, but also open up a path to uncharted territories in fundamental physics at ultra-high energies. The features of the signal can tell us further about non-Gaussianities or even parity-violation of Nature. On the other hand, non-detection could still constrain tensor perturbations, ruling out many

[11] The following discussions are mostly based on [19, 38].

[12] Acronym for the Deci-Hertz Interferometer Gravitational Wave Observatory.

large-field inflationary models.

History is often viewed in retrospect; we believe the *Golden Age of Cosmology* is still ahead of us.

Acknowledgement

The author thanks Anthony Challinor at the Department of Applied Mathematics and Theoretical Physics and the Institute of Astronomy, University of Cambridge for insightful discussions and valuable guidance.

References

[1] **CMBPol Study Team** Collaboration, D. Baumann *et al.*, "CMBPol Mission Concept Study: Probing Inflation with CMB Polarization," *AIP Conf. Proc.* **1141** (2009) 10–120, arXiv:0811.3919 [astro-ph].

[2] D. Baumann, "Cosmology - Part III Mathematical Tripos." Lecture notes, University of Cambridge. damtp.cam.ac.uk/user/db275/Cosmology/Lectures.pdf.

[3] D. Baumann, "Inflation," in *Physics of the large and the small, TASI 09, proceedings of the Theoretical Advanced Study Institute in Elementary Particle Physics*, pp. 523–686. 2011. arXiv:0907.5424 [hep-th].

[4] D. Baumann and H. V. Peiris, "Cosmological Inflation: Theory and Observations," *Adv. Sci. Lett.* **2** (2009) 105–120, arXiv:0810.3022 [astro-ph].

[5] W. Hu and M. J. White, ""cmb anisotropies: Total angular momentum method"," *Phys. Rev.* **D56** (1997) 596–615, arXiv:astro-ph/9702170 [astro-ph].

[6] A. Challinor, "Part-III Advanced Cosmology, Lecture notes: Physics of the cosmic microwave background." Lecture notes, University of Cambridge, 2017. Available upon request.

[7] A. Challinor and H. Peiris, "Lecture notes on the physics of cosmic microwave background anisotropies," in *American Institute of Physics Conference Series*, vol. 1132, pp. 86–140. 2009. arXiv:0903.5158 [astro-ph.CO].

[8] W. Hu and M. J. White, "A CMB polarization primer," *New Astron.* **2** (1997) 323, arXiv:astro-ph/9706147 [astro-ph].

[9] M. Kamionkowski, A. Kosowsky, and A. Stebbins, "A Probe of primordial gravity waves and vorticity," *Phys. Rev. Lett.* **78** (1997) 2058–2061, arXiv:astro-ph/9609132 [astro-ph].

[10] U. Seljak and M. Zaldarriaga, "Signature of gravity waves in polarization of the microwave background," *Phys. Rev. Lett.* **78** (1997) 2054–2057, arXiv:astro-ph/9609169 [astro-ph].

[11] J. Lizarraga, J. Urrestilla, D. Daverio, M. Hindmarsh, M. Kunz, and A. R. Liddle, "Constraining topological defects with temperature and polarization anisotropies," *Phys. Rev.* **D90** no. 10, (2014) 103504, arXiv:1408.4126 [astro-ph.CO].

[12] K. Jones-Smith, L. M. Krauss, and H. Mathur, "A Nearly Scale Invariant Spectrum of Gravitational Radiation from Global Phase Transitions," *Phys. Rev. Lett.* **100** (2008) 131302, arXiv:0712.0778 [astro-ph].

[13] R. Durrer, D. G. Figueroa, and M. Kunz, "Can Self-Ordering Scalar Fields explain the BICEP2 B-mode signal?," *JCAP* **1408** (2014) 029, arXiv:1404.3855 [astro-ph.CO].

[14] D. N. Spergel and M. Zaldarriaga, "CMB polarization as a direct test of inflation," *Phys. Rev. Lett.* **79** (1997) 2180–2183, arXiv:astro-ph/9705182 [astro-ph].

[15] A. Lewis, "CMB anisotropies from primordial inhomogeneous magnetic fields," *Phys. Rev.* **D70** (2004) 043011, arXiv:astro-ph/0406096 [astro-ph].

[16] M. Bucher, "Status of CMB observations in 2015," *Int. J. Mod. Phys. Conf. Ser.* **43** (2016) 1660188, arXiv:1606.03375 [astro-ph.CO].

[17] **Planck** Collaboration, P. A. R. Ade *et al.*, "Planck 2015 results. XX. Constraints on inflation," *Astron. Astrophys.* **594** (2016) A20, arXiv:1502.02114 [astro-ph.CO].

[18] E. M. Leitch, J. M. Kovac, C. Pryke, B. Reddall, E. S. Sandberg, M. Dragovan, J. E. Carlstrom, N. W. Halverson, and W. L. Holzapfel, "Measuring polarization with DASI," *Nature* **420** (2002) 763–771, arXiv:astro-ph/0209476 [astro-ph].

[19] C. Guzzetti, M., N. Bartolo, M. Liguori, and S. Matarrese, "Gravitational waves from inflation," *Riv. Nuovo Cim.* **39** no. 9, (2016) 399–495, arXiv:1605.01615 [astro-ph.CO].

[20] R. Kallosh, L. Kofman, and A. D. Linde, "Pyrotechnic universe," *Phys. Rev.* **D64** (2001) 123523, arXiv:hep-th/0104073 [hep-th].

[21] D. H. Lyth, "The Primordial curvature perturbation in the ekpyrotic universe," *Phys. Lett.* **B524** (2002) 1–4, arXiv:hep-ph/0106153 [hep-ph].

[22] E. I. Buchbinder, J. Khoury, and B. A. Ovrut, "Non-Gaussianities in new ekpyrotic cosmology," *Phys. Rev. Lett.* **100** (2008) 171302, arXiv:0710.5172 [hep-th].

[23] R. H. Brandenberger, S. Kanno, J. Soda, D. A. Easson, J. Khoury, P. Martineau, A. Nayeri, and S. P. Patil, "More on the spectrum of perturbations in string gas

cosmology," *JCAP* **0611** (2006) 009, arXiv:hep-th/0608186 [hep-th].

[24] N. Kaloper, L. Kofman, A. D. Linde, and V. Mukhanov, "On the new string theory inspired mechanism of generation of cosmological perturbations," *JCAP* **0610** (2006) 006, arXiv:hep-th/0608200 [hep-th].

[25] M. Gasperini and G. Veneziano, "The Pre - big bang scenario in string cosmology," *Phys. Rept.* **373** (2003) 1–212, arXiv:hep-th/0207130 [hep-th].

[26] N. Kaloper, A. D. Linde, and R. Bousso, "Pre - big bang requires the universe to be exponentially large from the very beginning," *Phys. Rev.* **D59** (1999) 043508, arXiv:hep-th/9801073 [hep-th].

[27] "The Acclerator Complex." [Online] CERN webpage. http://home.cern/about/accelerators.

[28] D. H. Lyth, "What would we learn by detecting a gravitational wave signal in the cosmic microwave background anisotropy?," *Phys. Rev. Lett.* **78** (1997) 1861–1863, arXiv:hep-ph/9606387 [hep-ph].

[29] **Planck** Collaboration, P. A. R. Ade *et al.*, "Planck 2015 results. XIII. Cosmological parameters," *Astron. Astrophys.* **594** (2016) A13, arXiv:1502.01589 [astro-ph.CO].

[30] **Planck** Collaboration, N. Aghanim *et al.*, "Planck 2015 results. XI. CMB power spectra, likelihoods, and robustness of parameters," *Astron. Astrophys.* **594** (2016) A11, arXiv:1507.02704 [astro-ph.CO].

[31] "Planck Mission Picture Gallery." [Online] ESA webpapage, Feb., 2015. https://www.cosmos.esa.int/web/planck/picture-gallery.

[32] M. Zaldarriaga and U. Seljak, "Gravitational lensing effect on cosmic microwave background polarization," *Phys. Rev.* **D58** (1998) 023003, arXiv:astro-ph/9803150 [astro-ph].

[33] **SPTpol** Collaboration, D. Hanson *et al.*, "Detection of B-mode Polarization in the Cosmic Microwave Background with Data from the South Pole Telescope," *Phys. Rev. Lett.* **111** no. 14, (2013) 141301, arXiv:1307.5830 [astro-ph.CO].

[34] **BICEP2** Collaboration, P. A. R. Ade *et al.*, ""detection of *b*-mode polarization at degree angular scales by bicep2"," *Phys. Rev. Lett.* **112** no. 24, (2014) 241101, arXiv:1403.3985 [astro-ph.CO].

[35] **BICEP2, Planck** Collaboration, P. A. R. Ade *et al.*, "Joint Analysis of BICEP2/Keck Array and Planck Data," *Phys. Rev. Lett.* **114** (2015) 101301, arXiv:1502.00612 [astro-ph.CO].

[36] L. Krauss, S. Dodelson, and S. Meyer, "Primordial Gravitational Waves and Cosmology," *Science* **328** (2010) 989–992, arXiv:1004.2504 [astro-ph.CO].

[37] W. H. Kinney, "TASI Lectures on Inflation," *ArXiv e-prints* (2009) , arXiv:0902.1529 [astro-ph.CO].

[38] J. Caligiuri and A. Kosowsky, "Inflationary Tensor Perturbations After BICEP2," *Phys. Rev. Lett.* **112** (2014) 191302, arXiv:1403.5324 [astro-ph.CO].

Appendices

We are reminded that in these appendices the convention adopted in § II.3 is in place: an overdot denotes a conformal time η-derivative.

A. Second Order Action for Gravitational Waves

A.1 Statement of the problem and set-ups

Problem — The action governing gravitational waves is the second order expansion of the full action

$$S = S_{\rm EH} + S_\phi \tag{109}$$

where the Einstein–Hilbert action is

$$S_{\rm EH} = \frac{M_{\rm Pl}^2}{2}\int {\rm d}^4x\,\sqrt{-g}R \tag{110}$$

and the matter action is

$$S_\phi = \int {\rm d}^4x\,\sqrt{-g}\mathcal{L}_\phi \tag{111}$$

with the scalar-field Lagrangian

$$\mathcal{L}_\phi = -\frac{1}{2}\partial_\mu\phi\partial^\mu\phi - V(\phi). \tag{112}$$

Set-up — The perturbed flat FLRW metric $g_{\mu\nu}$ is conformally equivalent to the perturbed Minkowski metric

$$g_{\mu\nu} = a(\eta)^2\bar{g}_{\mu\nu} = a(\eta)^2\left(\eta_{\mu\nu} + h_{\mu\nu}\right) \tag{113}$$

where the pure tensor perturbation $h_{\mu\nu}$ is spatial $h_{0\mu} \equiv 0$, traceless $\eta^{\mu\nu}h_{\mu\nu} = 0$ and transverse $\bar{\partial}_\mu h^{\mu\nu} = 0$. We will temporarily set $M_{\rm Pl} = 1$. The pre-superscript denotes the order of the quantity. Barred quantities are associated with the perturbed Minkowski metric, and unbarred associated with the perturbed FLRW metric, e.g. $\bar{\partial}^0 = -\partial_\eta$ but $\partial^0 = -a^{-2}\partial_\eta$.

A.2 Preliminary results

In deriving these results, we bear in mind that $h_{\mu\nu}$ is symmetric, purely-spatial, traceless and transverse; its indices are raised with the unperturbed Minkowski metric.

Result 1. The perturbed inverse Minkowski metric is

$$\bar{g}^{ab} = \eta^{ab} - h^{ab} + O\left(h^2\right), \tag{114}$$

and the perturbed inverse FLRW metric is $g^{ab} = a^{-2}\bar{g}^{ab}$.

Result 2. For conformally equivalent metrices $\tilde{g}_{ab} = \Omega^2 g_{ab}$, the associated Ricci scalars are related by

$$\tilde{R} = \Omega^{-2}\left(R - 6\nabla^2\ln\Omega - 6\nabla_a\ln\Omega\nabla^a\ln\Omega\right). \tag{115}$$

Proof. Since $\tilde{g}^{ab} = \Omega^{-2}g^{ab}$, direct computation gives

$$\begin{aligned}\tilde{\Gamma}^a{}_{bc} &= \frac{1}{2}\tilde{g}^{ad}\left(\partial_b\tilde{g}_{cd} + \partial_c\tilde{g}_{bd} - \partial_d\tilde{g}_{bc}\right)\\ &= \Gamma^a{}_{bc} + \frac{1}{2}\Omega^{-2}g^{ad}\left(\tilde{g}_{cd}\partial_b\Omega + \tilde{g}_{bd}\partial_c\Omega - \tilde{g}_{bc}\Omega\partial_d\right)\\ &= \tilde{\Gamma}^a{}_{bc} + \delta^a_c\partial_b\ln\Omega + \delta^a_b\partial_c\ln\Omega - g_{bc}\nabla^a\ln\Omega.\end{aligned}$$

Hence

$$\begin{aligned}\tilde{R}_{ab} &= \partial_c \tilde{\Gamma}^c{}_{ab} + \partial_b \tilde{\Gamma}^c{}_{ac} + \tilde{\Gamma}^c{}_{ab}\tilde{\Gamma}^d{}_{cd} - \tilde{\Gamma}^c{}_{ad}\tilde{\Gamma}^d{}_{bc} \\ &= R_{ab} - \partial_c\left(g_{ab}\nabla^c \ln\Omega\right) - 2\partial_a\partial_b \ln\Omega + 2\partial_a \ln\Omega\partial_b \ln\Omega \\ &\qquad + 2\Gamma^c{}_{ab}\,\partial_c \ln\Omega - 2g_{ab}\partial_c \ln\Omega\partial^c \ln\Omega \\ &\qquad - g_{ab}\Gamma^d{}_{cd}\,\nabla^c \ln\Omega + g_{bc}\Gamma^c{}_{ad}\,\nabla^d \ln\Omega + g_{ac}\Gamma^c{}_{bd}\,\nabla^d \ln\Omega.\end{aligned}$$

But

$$\begin{aligned}\partial_c\left(g_{ab}\nabla^c \ln\Omega\right) &= \nabla_c\left(g_{ab}\nabla^c \ln\Omega\right) + g_{bd}\Gamma^d{}_{ac}\,\nabla^c \ln\Omega + g_{ad}\Gamma^d{}_{bc}\,\nabla^c \ln\Omega - g_{ab}\Gamma^c{}_{cd}\,\nabla^d \ln\Omega \\ \partial_a\partial_b \ln\Omega &= \nabla_a\nabla_b \ln\Omega + \Gamma^c{}_{ab}\,\partial^c \ln\Omega\end{aligned}$$

so we have

$$\tilde{R}_{ab} = R_{ab} - 2\nabla_a\nabla_b \ln\Omega + 2\nabla_a \ln\Omega\nabla_b \ln\Omega - 2g_{ab}\nabla_c \ln\Omega\nabla^c \ln\Omega - g_{ab}\nabla^2 \ln\Omega.$$

Therefore

$$\begin{aligned}\tilde{R} &= \Omega^{-2}g^{ab}\tilde{R}_{ab} \\ &= \Omega^{-2}\left(R - 6\nabla^2 \ln\Omega - 6\nabla_a \ln\Omega\nabla^a \ln\Omega\right).\end{aligned}$$ □

Result 3. Using the formula

$$\det(X + \epsilon A) = \det X \det(I + \epsilon B) = \det X\left(1 + \epsilon \operatorname{tr} B + \frac{\epsilon^2}{2}\left[(\operatorname{tr} B)^2 - \operatorname{tr}\left(B^2\right)\right]\right) + O\left(\epsilon^3\right), \quad B \equiv X^{-1}A,$$

we have the perturbed FLRW metric determinant up to second order

$$\begin{aligned}{}^{(0)}g &= -a^8, \\ {}^{(1)}g &= {}^{(0)}g\ \operatorname{tr}\left({}^{(0)}g^{\mu\nu}\,a^2 h_{\nu\rho}\right) = {}^{(0)}g\ \operatorname{tr}\left(a^{-2}\eta^{\mu\nu}a^2 h_{\nu\rho}\right) = 0, \\ {}^{(2)}g &= \frac{1}{2}\,{}^{(0)}g\left[0^2 - \operatorname{tr}\left({}^{(0)}g^{\mu\nu}\,a^2 h_{\nu\rho}\ {}^{(0)}g^{\rho\sigma}\,a^2 h_{\sigma\lambda}\right)\right] = \frac{a^8}{2}h_{\mu\nu}h^{\mu\nu}.\end{aligned}$$

Thus using binomial expansion $\sqrt{-(g+\delta g)} = \sqrt{-g}\sqrt{1 + g^{-1}\,\delta g} = \sqrt{-g}\left[1 + \frac{1}{2}g^{-1}\,\delta g - \frac{1}{8}g^{-2}\,\delta g^2 + O\left(\delta g^3\right)\right]$,

$$\begin{aligned}{}^{(0)}\sqrt{-g} &= a^4, && (116)\\ {}^{(1)}\sqrt{-g} &= \frac{1}{2}\,{}^{(0)}\sqrt{-g}\ {}^{(0)}g^{-1}\ {}^{(1)}g = 0, && (117)\\ {}^{(2)}\sqrt{-g} &= \frac{1}{2}\,{}^{(0)}\sqrt{-g}\ {}^{(0)}g^{-1}\ {}^{(2)}g = -\frac{a^4}{4}h_{\mu\nu}h^{\mu\nu}. && (118)\end{aligned}$$

Result 4. The perturbed Minkowski metric Christoffel symbols up to second order are

$$\begin{aligned}\bar{\Gamma}^0{}_{ij} &= \frac{1}{2}\dot{h}_{ij}, \\ \bar{\Gamma}^i{}_{j0} &= \frac{1}{2}\left(\dot{h}^i{}_j - h^{ik}\dot{h}_{kj}\right) + O\left(h^3\right), \\ \bar{\Gamma}^i{}_{jk} &= \frac{1}{2}\left(\bar{\partial}_j h^i{}_k + \bar{\partial}_k h^i{}_j - \bar{\partial}^i h_{jk} - h^{il}\bar{\partial}_j h_{lk} - h^{il}\bar{\partial}_k h_{lj} + h^{il}\bar{\partial}_l h_{jk}\right) + O\left(h^3\right)\end{aligned} \tag{119}$$

and all others are identically zero to all orders.

Result 5. We compute the following quantities up to second order

$$\begin{aligned}
\bar{g}^{\mu\nu}\bar{\partial}_\rho\bar{\Gamma}^\rho{}_{\mu\nu} &= -\frac{1}{2}h^{ij}\ddot{h}_{ij} + \frac{1}{2}h^{jk}\bar{\partial}^i\bar{\partial}_i h_{jk},\\
-\bar{g}^{\mu\nu}\bar{\partial}_\nu\bar{\Gamma}^\rho{}_{\mu\rho} &= -\frac{1}{2}\partial_\eta\left(h^{ij}\partial_\eta h_{ij}\right) + \frac{1}{2}\ddot{h}_{ij} + \frac{1}{2}\bar{\partial}^k\left(h^{ij}\bar{\partial}_k h_{ij}\right),\\
\bar{g}^{\mu\nu}\bar{\Gamma}^\rho{}_{\mu\nu}\bar{\Gamma}^\sigma{}_{\rho\sigma} &= 0,\\
-\bar{g}^{\mu\nu}\bar{\Gamma}^\sigma{}_{\mu\rho}\bar{\Gamma}^\rho{}_{\nu\sigma} &= -\frac{1}{4}\dot{h}_{ij}\dot{h}^{ij} + \frac{1}{4}\bar{\partial}_i h_{jk}\bar{\partial}^i h^{jk}
\end{aligned}$$

which add up to give the perturbed Minkowski metric Ricci scalar up to second order

$$\bar{R} = -h^{ij}\ddot{h}_{ij} - \frac{1}{4}\bar{\partial}_i h_{jk}\bar{\partial}^i h^{jk} - \frac{3}{4}\dot{h}_{ij}\dot{h}^{ij} \tag{120}$$

Result 6. Combining Result 2 using the conformal factor $\Omega = a$, Result 4 and Result 5, we extract the perturbed FLRW metric Ricci scalar up to second order

$$\begin{aligned}
{}^{(0)}R &= -\frac{6}{a^2}\left(-\partial_\eta^2 \ln a - a^{-2}\dot{a}^2\right) = \frac{6}{a^2}(\mathcal{H}' + \mathcal{H}), && (121)\\
{}^{(1)}R &= 0, && (122)\\
{}^{(2)}R &= -a^{-2}\left(h^{ij}\ddot{h}_{ij} + \frac{1}{4}\bar{\partial}_i h_{jk}\bar{\partial}^i h^{jk} + \frac{3}{4}\dot{h}_{ij}\dot{h}^{ij}\right) - 6a^{-2}\,{}^{(2)}\bar{\Gamma}^i{}_{i0}\,\bar{\partial}^0 \ln a\\
&= -a^{-2}\left(h^{ij}\ddot{h}_{ij} + \frac{1}{4}\bar{\partial}_i h_{jk}\bar{\partial}^i h^{jk} + \frac{3}{4}\dot{h}_{ij}\dot{h}^{ij}\right) - 3a^{-2}\mathcal{H}h^{ij}\dot{h}_{ij}. && (123)
\end{aligned}$$

A.3 Full calculations

Einstein–Hilbert action — We need to calculate the second order quantity which by Eqn. (117) is just

$${}^{(2)}\left(\sqrt{-g}R\right) = {}^{(0)}\sqrt{-g}\;{}^{(2)}R + {}^{(2)}\sqrt{-g}\;{}^{(0)}R\,.$$

By Eqns. (116) and (123)

$${}^{(0)}\sqrt{-g}\;{}^{(2)}R = -a^2\left(h^{ij}\ddot{h}_{ij} + \frac{1}{4}\bar{\partial}_i h_{jk}\bar{\partial}^i h^{jk} + \frac{3}{4}\dot{h}_{ij}\dot{h}^{ij}\right) - 3a^2\mathcal{H}h^{ij}\dot{h}_{ij}.$$

Integrating the first term by parts,

$$-\int \mathrm{d}^4x\, a^2 h^{ij}\ddot{h}_{ij} = \int \mathrm{d}^4x\, 2a^2\mathcal{H}h^{ij}\dot{h}_{ij} + \int \mathrm{d}^4x\, a^2\dot{h}^{ij}\dot{h}_{ij},$$

we find the integral

$$\int \mathrm{d}^4x\;{}^{(0)}\sqrt{-g}\;{}^{(2)}R = \frac{1}{4}\int \mathrm{d}^4x\, a^2\dot{h}^{ij}\dot{h}_{ij} - \frac{1}{4}\int \mathrm{d}^4x\, a^2\bar{\partial}_i h_{jk}\bar{\partial}^i h^{jk} - \int \mathrm{d}^4x\, a^2\mathcal{H}h^{ij}\dot{h}_{ij}.$$

Integrate the last term by parts

$$\begin{aligned}
-\int \mathrm{d}^4x\, a^2\mathcal{H}h^{ij}\dot{h}_{ij} &= \frac{1}{2}\int \mathrm{d}^4x\, \partial_\eta\left(a^2\mathcal{H}\right)h^{ij}h_{ij}\\
&= \frac{1}{2}\int \mathrm{d}^4x\, a^2\left(\dot{\mathcal{H}} + 2\mathcal{H}^2\right).
\end{aligned}$$

Next we have from Eqns. (118) and (121)

$${}^{(2)}\sqrt{-g}\;{}^{(0)}R = -\frac{3}{2}\int \mathrm{d}^4x\, a^2(\dot{\mathcal{H}} + \mathcal{H}^2)h_{ij}h^{ij}.$$

We now arrive at

$$^{(2)}S_{\rm EH} = \frac{1}{8}\int \mathrm{d}^4x\, a^2 \dot{h}_{ij}\dot{h}^{ij} - \frac{1}{8}\int \mathrm{d}^4x\, a^2 \bar{\partial}_i h_{jk}\bar{\partial}^i h^{jk} - \frac{1}{4}\int \mathrm{d}^4x\, a^2\left(\mathcal{H}^2 + 2\dot{\mathcal{H}}\right)h_{ij}h^{ij}. \tag{124}$$

Matter action — We need to calculate the second order quantity which by Eqn. (117) is just

$$^{(2)}(\sqrt{-g}\mathcal{L}_\phi) = {}^{(2)}\sqrt{-g}\ {}^{(0)}\mathcal{L}_\phi + {}^{(0)}\sqrt{-g}\ {}^{(2)}\mathcal{L}_\phi\,.$$

Since $\phi \equiv \phi(t)$,

$$^{(2)}\mathcal{L}_\phi \equiv {}^{(2)}\left[-\frac{1}{2}g^{\mu\nu}\partial_\mu\phi\partial_\nu\phi - V(\phi)\right] = -\frac{1}{2}\ {}^{(2)}g^{\mu\nu}\,\partial_\mu\phi\partial_\nu\phi = -\frac{a^{-4}}{2}h^{ik}h^j{}_k\partial_i\phi\partial_j\phi = 0$$

and we have from Eqn. (118)

$$^{(2)}(\sqrt{-g}\mathcal{L}_\phi) = {}^{(2)}\sqrt{-g}\ {}^{(0)}\mathcal{L}_\phi = -\frac{a^4}{4}h_{ij}h^{ij}\left[\frac{1}{2}a^{-2}\dot{\phi}^2 - V(\phi)\right].$$

But by the Friedman equations (3) written in terms of conformal time

$$\begin{aligned} 3\mathcal{H}^2 &= a^2\rho, \\ -6\dot{\mathcal{H}} &= a^2(\rho + 3P) \end{aligned}$$

where $\rho = \dot{\phi}^2/(2a^2) + V$ and $P = \dot{\phi}^2/(2a^2) - V$, we have

$$^{(2)}(\sqrt{-g}\mathcal{L}_\phi) = {}^{(2)}\sqrt{-g}\ {}^{(0)}\mathcal{L}_\phi = -\frac{a^4}{4}h_{ij}h^{ij}P = \frac{a^2}{4}h_{ij}h^{ij}\left(\mathcal{H}^2 + 2\dot{\mathcal{H}}\right).$$

Therefore we arrive at

$$^{(2)}S_\phi = \frac{1}{4}\int \mathrm{d}^4x\, a^2\left(\mathcal{H}^2 + 2\dot{\mathcal{H}}\right)h_{ij}h^{ij}. \tag{125}$$

Finally, adding the two sectors [Eqns. (124) and (125)] together and restoring $M_{\rm Pl}$, we obtain

$$^{(2)}S = \frac{M_{\rm Pl}^2}{8}\int \mathrm{d}\eta\, \mathrm{d}^3x\, a^2\left(\dot{h}_{ij}\dot{h}^{ij} - \bar{\partial}_i h_{jk}\bar{\partial}^i h^{jk}\right). \tag{126}$$

This is precisely Eqn. (36) where the derivatives are taken with respect to the Minkowski metric.

A.4 Extension

In general, the energy-momentum tensor for a single scalar field is

$$T^{\mu\nu} = \partial^\mu\phi\partial^\nu\phi + g^{\mu\nu}\mathcal{L}_\phi \tag{127}$$

so Eqn. (1) gives $P = {}^{(0)}\mathcal{L}_\phi$ as we saw above. Equivalently the matter action (111) can be recast as [1]

$$\mathcal{L}_\phi = \int \mathrm{d}^4x\, \sqrt{-g}P(X,\phi) \tag{128}$$

where pressure P is a function of both the inflaton field and the kinetic term $X \equiv -g^{\mu\nu}\partial_\mu\phi\partial_\nu\phi/2$. Proceeding as above with the substitution of the Friedman equations yields the same second order action for gravitational waves in FLRW background spacetime, but now valid for more general single-field inflation minimally coupled to gravity where the kinetic terms include only first derivatives.

B. Evolution of Gravitational Waves

The non-zero Christoffel symbols for the perturbed metric (29) are, to first order,

$$\begin{aligned}
\Gamma^0{}_{00} &= \mathcal{H}, \\
\Gamma^0{}_{ij} &= \mathcal{H}\left(\delta_{ij} + h_{ij}\right) + \frac{1}{2}\dot{h}_{ij}, \\
\Gamma^i{}_{j0} &= \mathcal{H}\delta^i_j + \frac{1}{2}\dot{h}^i{}_j, \\
\Gamma^i{}_{jk} &= \frac{1}{2}\left(\partial_j h^i{}_k + \partial_k h^i{}_j - \partial^i h_{jk}\right).
\end{aligned} \tag{129}$$

Observing that the Ricci scalar $R = g^{\mu\nu}R_{\mu\nu}$ does not receive linear-order contributions from tensor perturbations as h_{ij} is transverse, we have

$$R = \frac{6}{a^2}\left(\dot{\mathcal{H}} + \mathcal{H}^2\right)$$

equal to its value for the unperturbed FLRW metric. For convenience, we first compute the following results

$$\Gamma^\rho{}_{0\rho} = 4\mathcal{H}, \quad \Gamma^\rho{}_{i\rho} = 0,$$

so that the Ricci tensor is

$$\begin{aligned}
R_{ij} &= \partial_0\Gamma^0{}_{ij} + \partial_k\Gamma^k{}_{ij} - \partial_j\Gamma^\rho{}_{i\rho} + \Gamma^0{}_{ij}\Gamma^\rho{}_{0\rho} - \Gamma^0{}_{ik}\Gamma^k{}_{j0} - \Gamma^k{}_{i0}\Gamma^0{}_{jk} - \Gamma^k{}_{il}\Gamma^l{}_{jk} \\
&= \left(\dot{\mathcal{H}} + 2\mathcal{H}^2\right)\left(\delta_{ij} + h_{ij}\right) + \frac{1}{2}\left(\ddot{h}_{ij} - \nabla^2 h_{ij} + 2\mathcal{H}\dot{h}_{ij}\right) + (\mathcal{H}' + 2\mathcal{H}^2)h_{ij}
\end{aligned}$$

and the Einstein tensor is

$$G_{ij} \equiv R_{ij} - \frac{1}{2}g_{ij}R = -\left(2\dot{\mathcal{H}} + \mathcal{H}^2\right)\delta_{ij} + \underbrace{\frac{1}{2}\left(\ddot{h}_{ij} - \nabla^2 h_{ij} + 2\mathcal{H}\dot{h}_{ij}\right) - \left(2\dot{\mathcal{H}} + \mathcal{H}^2\right)h_{ij}}_{=\delta G_{ij}} \tag{130}$$

all at the linear order.

On the other hand, we must also calculate the tensor perturbation to the energy-momentum contribution, which for a perfect fluid is

$$T_{\mu\nu} = (\rho + P)U_\mu U_\nu + Pg_{\mu\nu} + a^2\Pi_{ij}$$

where ρ, P, and Π_{ij} are the density, pressure and anisotropic stress of the fluid, and U^μ its 4-velocity (a first order quantity). Substitution of the perturbations $\rho = \bar{\rho} + \delta\rho$, $P = \bar{P} + \delta P$ into the energy-momentum tensor above yields the first order perturbation

$$\delta T_{ij} = a^2\bar{P}h_{ij} + a^2\Pi_{ij}. \tag{131}$$

Applying the Einstein field equation to quantities (130) and (131), employing the background Friedman equation [see Eqns. (3) and (4)] $2\dot{\mathcal{H}} + \mathcal{H}^2 = -M_{\rm Pl}^{-2}a^2\bar{P}$ and ignoring anisotropic stress Π_{ij}, we obtain the ij-component of the Einstein equation for the evolution of gravitational waves

$$\ddot{h}_{ij} + 2\mathcal{H}\dot{h}_{ij} - \nabla^2 h_{ij} = 0$$

which in Fourier space is precisely Eqn. (45) for each polarisation state.

Example 1 (Evolution in the matter-dominated era). During matter domination, $\mathcal{H} = 2/\eta$ so the equation above becomes

$$\ddot{h}^{(p)} + \frac{4}{\eta}\dot{h}^{(p)} + k^2 h^{(p)} = 0 \tag{132}$$

which we recognise as a (spherical) Bessel equation after making the change of variables $x \equiv k\eta$, $h \equiv f(x)/x$,

$$x^2\frac{\mathrm{d}^2 f}{\mathrm{d}x^2} + 2x\frac{\mathrm{d}f}{\mathrm{d}x} + (x^2 - 2)f = 0$$

so the solution is simply the spherical Bessel function $f(x) = j_1(x)$. Thus the solution is

$$h^{(p)}(\eta, \mathbf{k}) = 3h^{(p)}(\mathbf{k})\frac{j_1(k\eta)}{k\eta}. \tag{133}$$

Either by differentiating Eqn. (132) above to obtain a new Bessel equation, or using the Bessel function property

$$j_{n+1}(x) = -(-x)^n \frac{\mathrm{d}}{\mathrm{d}x}(-x)^{-n} j_n(x),$$

we obtain the gravitational wave shear

$$\dot{h}^{(p)}(\eta, \mathbf{k}) = -3h^{(p)}(\mathbf{k})\frac{j_2(k\eta)}{\eta}.$$

Example 2 (Asymptotic features for general $a(\eta)$). Outside the Hubble horizon $k \ll \mathcal{H}$, it is straight-forward to see $h^{(\pm 2)} = \text{const.}$ is the growing solution for Eqn. (45). Since we can rewrite Eqn. (45) as

$$\partial_\eta^2\left(ah^{(\pm 2)}\right) + \left(k^2 - \frac{\ddot{a}}{a}\right)ah^{(\pm 2)} = 0, \tag{134}$$

for modes well inside the Hubble horizon $k \gg \mathcal{H}$, we can neglect $\ddot{a}/a \ll k^2$, thus obtaining

$$h^{(\pm 2)} \propto \frac{\mathrm{e}^{\mathrm{i}k\eta}}{a}.$$

This is interpreted as the usual gravitational waves in flat Minkowski spacetime, but with a damping factor a: the radiation nature of gravitons means the energy density averaged over many oscillations $a^{-2}\left\langle \ddot{h}_{ij}\ddot{h}^{ij}\right\rangle \propto a^{-4}$, so that we have adiabatic decay $h_{ij} \propto a^{-1}$.

C. Rotations via the Wigner D-Matrix

A 3-dimensional rotation can be completely specified by the Euler angles (α, β, γ). For a general rotation of the spherical harmonics, we act with the operator

$$\hat{D}(\alpha, \beta, \gamma) = \mathrm{e}^{-\mathrm{i}\alpha\hat{L}_z}\,\mathrm{e}^{-\mathrm{i}\beta\hat{L}_y}\,\mathrm{e}^{-\mathrm{i}\gamma\hat{L}_z}$$

where $\hat{L}_i$ are the angular momentum operators (generators of the rotation), so that $\hat{D}Y_{\ell m} = \sum_{m'} D^{\ell}_{m'm}Y_{\ell m'}$ is an expansion in the basis of the spherical harmonics. The coefficients $D^{\ell}_{m'm}$ are the components of the *Wigner D-matrices*.

The rotation operators are unitary,

$$\hat{D}^\dagger\hat{D} = \mathbb{I} \quad \Longrightarrow \quad \sum_n D^{\ell *}_{nm}D^{\ell}_{nm'} = \delta_{mm'},$$

and under an active rotation, the spherical multipole coefficients of a random field on a sphere transform as

$$\begin{aligned} f_{\ell m} &\longrightarrow \int \mathrm{d}\hat{\mathbf{n}}\, Y^*_{\ell m}\hat{D}\sum_{\ell', m'} f_{\ell' m'}Y_{\ell' m'} \\ &= \int \mathrm{d}\hat{\mathbf{n}}\, Y^*_{\ell m}\sum_{\ell', m', n'} f_{\ell' m'}D^{\ell'}_{n' m'}Y_{\ell' n'} \\ &= \sum_{m'} D^{\ell}_{m m'}f_{\ell m'} \end{aligned}$$

by the orthogonality relation of the spherical harmonics

$$\int \mathrm{d}\hat{\mathbf{n}}\, Y_{\ell m}Y^*_{\ell' m'} = \delta_{\ell\ell'}\delta_{mm'}.$$

An explicit result for the Wigner D-matrix is that

$$D^{\ell}_{m0}(\phi, \theta, 0) = \sqrt{\frac{4\pi}{2\ell + 1}}Y^*_{\ell m}(\hat{\mathbf{n}})$$

which could be derived from $Y_{\ell m}(\hat{\mathbf{z}}) = \sqrt{(2\ell + 1)/(4\pi)}\delta_{m0}$ [6].

D. The Geodesic Equation for Tensor Perturbations

The first order metric connections can be found in Eqn. (129) in Appendix B.

With the tetrad given in Eqn. (56), we have

$$\frac{\mathrm{d}x^\mu}{\mathrm{d}\lambda} = p^\mu = \frac{\epsilon}{a^2}\left(1, e^{\hat{i}} - \frac{1}{2}h^i{}_j e^{\hat{j}}\right)$$

where λ is the affine parameter, so that

$$\frac{\mathrm{d}\eta}{\mathrm{d}\lambda} = \frac{\epsilon}{a^2}, \quad \frac{\mathrm{d}x^i}{\mathrm{d}\eta} = e^{\hat{i}} - \frac{1}{2}h^i{}_j e^{\hat{j}}$$

to linear order. The time-component of the geodesic equation

$$\frac{\epsilon}{a^2}\frac{\mathrm{d}p^\mu}{\mathrm{d}\eta} + \Gamma^\mu{}_{\nu\rho}p^\nu p^\rho = 0$$

is then

$$\frac{\epsilon}{a^2}\frac{\mathrm{d}}{\mathrm{d}\eta}\frac{\epsilon}{a^2} + \left(\frac{\epsilon}{a^2}\right)^2\left[\mathcal{H} + \mathcal{H}\left(\delta_{ij} + h_{ij} + \frac{1}{2}\dot{h}_{ij}\right)\left(e^{\hat{i}} - \frac{1}{2}h^i{}_k e^{\hat{k}}\right)\left(e^{\hat{j}} - \frac{1}{2}h^j{}_l e^{\hat{l}}\right)\right] = 0$$

from which the linear-order terms can be extracted

$$\frac{\mathrm{d}\ln\epsilon}{\mathrm{d}\eta} + \left(\mathcal{H}h_{ij} + \frac{1}{2}\dot{h}_{ij}\right)e^{\hat{i}}e^{\hat{j}} - \mathcal{H}h_{ij}e^{\hat{i}}e^{\hat{j}} = 0$$

which is precisely Eqn. (57).

E. Calculation of the Gravitational Shear Contribution to Temperature Anisotropies

The calculations in this appendix primarily follows that in [6]. To derive Eqn. (60) from Eqn. (59) modulated by a plane wave due to the evolution of gravitational waves, we first use the *Rayleigh plane-wave expansion*

$$\mathrm{e}^{-\mathrm{i}\chi\mathbf{k}\cdot\mathbf{e}} = \sum_{L\geqslant 0}(-\mathrm{i})^L(2L+1)j_L(k\chi)P_L(\cos\theta) \tag{135}$$

and $P_L(\cos\theta) = \sqrt{4\pi/(2L+1)}Y_{L0}(\mathbf{e})$ to rewrite it as

$$\sqrt{\frac{4\pi}{15}}\dot{h}^{(\pm 2)}(\eta, k\hat{\mathbf{z}})Y_{2\pm 2}(\mathbf{e})\,\mathrm{e}^{-\mathrm{i}k\chi\cos\theta} = \frac{4\pi}{\sqrt{15}}\dot{h}^{(\pm 2)}(\eta, k\hat{\mathbf{z}})\sum_{L\geqslant 0}(-\mathrm{i})^L\sqrt{2L+1}j_L(k\chi)Y_{2\pm 2}(\mathbf{e})Y_{L0}(\mathbf{e}).$$

The product of two spherical harmonics can be expanded in the basis of spherical harmonics with Wigner $3j$-symbol valued coefficients

$$Y_{2\pm 2}(\mathbf{e})Y_{L0}(\mathbf{e}) = \sum_{\ell,m}\sqrt{\frac{5(2L+1)(2\ell+1)}{4\pi}}\begin{pmatrix} 2 & L & \ell \\ \pm 2 & 0 & m\end{pmatrix}\begin{pmatrix} 2 & L & \ell \\ 0 & 0 & 0\end{pmatrix}Y^*_{\ell m}(\mathbf{e})$$

but for temperature anisotropies, $m = \pm 2$ and thus $\ell \geqslant 2$, so

$$\sqrt{\frac{4\pi}{15}}\dot{h}^{(\pm 2)}(\eta, k\hat{\mathbf{z}})Y_{2\pm 2}(\mathbf{e})\,\mathrm{e}^{-\mathrm{i}k\chi\cos\theta} = \sqrt{\frac{4\pi}{3}}\dot{h}^{(\pm 2)}(\eta, k\hat{\mathbf{z}})\sum_{L\geqslant 0}(-\mathrm{i})^L(2L+1)j_L(k\chi)\sum_{\ell\geqslant 2}\sqrt{2\ell+1}\begin{pmatrix} 2 & L & \ell \\ \mp 2 & 0 & \pm 2\end{pmatrix}\begin{pmatrix} 2 & L & \ell \\ 0 & 0 & 0\end{pmatrix}Y_{\ell\pm 2}(\mathbf{e})$$

where we have used the reality condition $Y^*_{\ell\pm 2} = (-1)^{\pm 2}Y_{\ell\mp 2}$.

We shall concentrate on the summation over L, i.e. the expression

$$\sum_{L\geqslant 0}(-\mathrm{i})^L(2L+1)j_L(k\chi)\begin{pmatrix}2 & L & \ell\\ \mp 2 & 0 & \pm 2\end{pmatrix}\begin{pmatrix}2 & L & \ell\\ 0 & 0 & 0\end{pmatrix}.$$

The Wigner $3j$-symbol $\begin{pmatrix}2 & L & \ell\\ 0 & 0 & 0\end{pmatrix}$ is non-vanishing only for $L+\ell\in 2\mathbb{Z}$ by the time-reversal formula

$$\begin{pmatrix}a & b & c\\ -d & -e & -f\end{pmatrix}=(-1)^{a+b+c}\begin{pmatrix}a & b & c\\ d & e & f\end{pmatrix}, \tag{136}$$

hence the summation in L is only over $L=\ell,\ell\pm 2$ by triangle inequality $|a-b|\leqslant c\leqslant a+b$ of the Wigner $3j$-symbol $\begin{pmatrix}a & b & c\\ d & e & f\end{pmatrix}$. We receive the following contributions

$$A\coloneqq(-\mathrm{i})^{\ell+2}(2\ell+5)j_{\ell+2}(x)\begin{pmatrix}2 & \ell+2 & \ell\\ \mp 2 & 0 & \pm 2\end{pmatrix}\begin{pmatrix}2 & \ell+2 & \ell\\ 0 & 0 & 0\end{pmatrix}=-(-\mathrm{i})^{\ell}\sqrt{\frac{3}{8}}\sqrt{\frac{(\ell+2)!}{(\ell-2)!}}\frac{1}{(2\ell+3)(2\ell+1)}j_{\ell+2}(x)$$

and similarly

$$B\coloneqq-(-\mathrm{i})^{\ell}\sqrt{\frac{3}{8}}\sqrt{\frac{(\ell+2)!}{(\ell-2)!}}\frac{1}{(2\ell+1)(2\ell-1)}j_{\ell-2}(x),\quad C\coloneqq-(-\mathrm{i})^{\ell}\sqrt{\frac{3}{8}}\sqrt{\frac{(\ell+2)!}{(\ell-2)!}}\frac{2}{(2\ell+3)(2\ell-1)}j_{\ell}(x)$$

where $x\equiv k\chi$ and we have used the following results

$$\begin{aligned}\begin{pmatrix}2 & \ell+2 & \ell\\ \pm 2 & 0 & \mp 2\end{pmatrix}\begin{pmatrix}2 & \ell+2 & \ell\\ 0 & 0 & 0\end{pmatrix}&=\sqrt{\frac{3}{8}}\sqrt{\frac{(\ell+2)!}{(\ell-2)!}}\frac{1}{(2\ell+5)(2\ell+3)(2\ell+1)},\\ \begin{pmatrix}2 & \ell-2 & \ell\\ \pm 2 & 0 & \mp 2\end{pmatrix}\begin{pmatrix}2 & \ell-2 & \ell\\ 0 & 0 & 0\end{pmatrix}&=\sqrt{\frac{3}{8}}\sqrt{\frac{(\ell+2)!}{(\ell-2)!}}\frac{1}{(2\ell+1)(2\ell-1)(2\ell-3)},\\ \begin{pmatrix}2 & \ell & \ell\\ \pm 2 & 0 & \mp 2\end{pmatrix}\begin{pmatrix}2 & \ell & \ell\\ 0 & 0 & 0\end{pmatrix}&=-\sqrt{\frac{3}{2}}\sqrt{\frac{(\ell+2)!}{(\ell-2)!}}\frac{1}{(2\ell+3)(2\ell+1)(2\ell-1)}.\end{aligned}$$

We utilise the recursion relation for $j_\ell(x)$,

$$\begin{aligned}j_\ell&=\frac{x}{2\ell+1}(j_{\ell+1}+j_{\ell-1})\\ &=\frac{x}{2\ell+1}\left[\frac{x}{2\ell+3}(j_{\ell+2}+j_\ell)+\frac{x}{2\ell-1}(j_\ell+j_{\ell-2})\right]\\ &=\frac{x^2}{(2\ell+1)(2\ell+3)}j_{\ell+2}+\frac{x^2}{(2\ell-1)(2\ell+1)}j_{\ell-2}+\frac{x^2}{2\ell+1}\left(\frac{1}{2\ell+3}+\frac{1}{2\ell-1}\right)j_\ell\end{aligned} \tag{137}$$

so $(2\ell+3)(2\ell+1)(2\ell-1)j_\ell=x^2\left[(2\ell-1)j_{\ell+2}+(2\ell+3)j_{\ell-2}+(4\ell+2)j_\ell\right]$. Therefore the total contribution of A, B and C gives

$$\dot{h}_{ij}^{(\pm 2)}(\eta,k\hat{\mathbf{z}})e^{\hat{i}}e^{\hat{j}}\,\mathrm{e}^{-\mathrm{i}k\chi\cos\theta}=-\sqrt{\frac{\pi}{2}}\dot{h}^{(\pm 2)}(\eta,k\hat{\mathbf{z}})\sum_{\ell\geqslant 2}(-\mathrm{i})^{\ell}\sqrt{2\ell+1}\sqrt{\frac{(\ell+2)!}{(\ell-2)!}}\frac{j_\ell(k\chi)}{(k\chi)^2}Y_{\ell\pm 2}(\mathbf{e}).$$

F. Properties of Spin Spherical Harmonics

We list below a number of properties of the spin spherical harmonics:

- Orthogonality relation

$$\int \mathrm{d}\hat{\mathbf{n}}\;{}_sY_{\ell m s}Y^*_{\ell' m'}=\delta_{\ell\ell'}\delta_{mm'}; \tag{138}$$

- Conjugation relation

$$ {}_sY^*_{\ell m} = (-1)^{s+m}\,{}_{-s}Y_{\ell -m}\,; \tag{139} $$

- Parity relation

$$ {}_sY_{\ell m}(-\hat{\mathbf{n}}) = (-1)^{\ell}\,{}_{-s}Y_{\ell m}(\hat{\mathbf{n}}); \tag{140} $$

- Wigner D-matrix relation

$$ D^{\ell}_{-m\,s}(\phi,\theta,0) = (-1)^m\sqrt{\frac{4\pi}{2\ell+1}}\,{}_sY_{\ell m}(\theta,\phi); \tag{141} $$

- Product formula

$$ {}_{s_1}Y_{\ell_1 m_1}\,{}_{s_2}Y_{\ell_2 m_2} = \sum_{L,M,S}(-1)^{\ell_1+\ell_2+L}\sqrt{\frac{(2\ell_1+1)(2\ell_2+1)(2L+1)}{4\pi}}\begin{pmatrix}\ell_1 & \ell_2 & L\\ m_1 & m_2 & M\end{pmatrix}\begin{pmatrix}\ell_1 & \ell_2 & L\\ s_1 & s_2 & S\end{pmatrix}{}_sY_{LM}\,. \tag{142} $$

G. Tensor Calculus on the 2-Sphere

This mathematical introduction to tensor calculus on the 2-sphere may be found in literatures such as [6]. In a basis of complex null vectors on the 2-sphere, we decompose the metric tensor and the alternating tensor as

$$ g_{ab} = \frac{1}{2}(m_{+a}m_{-b} + m_{-a}m_{+b}), \quad \varepsilon_{ab} = \frac{\mathrm{i}}{2}(m_{+a}m_{-b} - m_{-a}m_{+b}). \tag{143} $$

The action of the alternating tensor on the null basis vectors is a rotation by $\pi/2$:

$$ \varepsilon_a{}^b m_{\pm b} = \pm\mathrm{i}m_{\pm a}. \tag{144} $$

We can express $m^a_\pm$ in the spherical polar coordinate basis as Eqn. (72). They satisfy the parallel transport equations

$$ m^a_+\nabla_a m^b_\pm = \pm\cot\theta m^b_\pm, \quad m^a_-\nabla_a m^b_\pm = \mp\cot\theta m^b_\pm. \tag{145} $$

To derive Eqn. (76) from Eqns. (74) and (75), we write

$$ \begin{aligned} Q \pm \mathrm{i}U &= m^a_\pm m^b_\pm\Big[\nabla_{\langle a}\nabla_{b\rangle}P_E + \varepsilon^c{}_{(a}\nabla_{b)}\nabla_c P_B\Big] \\ &= m^a_\pm m^b_\pm\nabla_a\nabla_b(P_E \pm \mathrm{i}P_B) \\ &= \Big[\left(m^a_\pm\nabla_a\right)^2 - \underbrace{m^a_\pm\left(\nabla_a m^b_\pm\right)}_{=\cot\theta m^b_\pm}\nabla_b\Big](P_E \pm \mathrm{i}P_B) \\ &= \Big[(\partial_\theta \pm \mathrm{i}\,\mathrm{cosec}\,\theta\partial_\phi)^2 - \cot\theta(\partial_\theta \pm \mathrm{i}\,\mathrm{cosec}\,\theta\partial_\phi)\Big](P_E \pm \mathrm{i}P_B) \\ &= \sin\theta(\partial_\theta \pm \mathrm{i}\,\mathrm{cosec}\,\theta\partial_\phi)\Big[(\sin\theta)^{-1}(\partial_\theta \pm \mathrm{i}\,\mathrm{cosec}\,\theta\partial_\phi)(P_E \pm \mathrm{i}P_B)\Big] \end{aligned} $$

which we recognise by Eqn. (70) as

$$ Q + \mathrm{i}U = \eth\,\eth(P_E + \mathrm{i}P_B), \quad Q - \mathrm{i}U = \bar{\eth}\,\bar{\eth}(P_E - \mathrm{i}P_B). $$

H. Calculation of the Gravitational Shear Contribution to Temperature Anisotropies

The calculations in this appendix primarily follows that in [6]. To derive Eqn. (83) from Eqn. (82), we note only $m = p$ summands survive in Eqn. (82). Employing the Rayleigh plane-wave expansion [cf. Eqn. (135)]

$$
\begin{aligned}
&(Q \pm \mathrm{i}U)(\eta_0, k\hat{\mathbf{z}}, \mathbf{e}) \\
&\quad \propto \mathrm{e}^{-\mathrm{i}k\chi_* \cos\theta}\, {}_{\pm 2}Y_{2p}(\mathbf{e}) \\
&\quad = {}_{\pm 2}Y_{2p}(\mathbf{e}) \sum_L \sqrt{4\pi(2L+1)}(-\mathrm{i})^L j_L(k\chi_*) Y_{L0}(\mathbf{e}) \\
&\quad = \sum_L \sqrt{4\pi(2L+1)}(-\mathrm{i})^L j_L(k\chi_*) \sum_{\ell,m,s} (-1)^{2+L+\ell} \sqrt{\frac{5(2L+1)(2\ell+1)}{4\pi}} \begin{pmatrix} 2 & L & \ell \\ p & 0 & m \end{pmatrix} \begin{pmatrix} 2 & L & \ell \\ \pm 2 & 0 & s \end{pmatrix} {}_s Y^*_{\ell m}(\mathbf{e}) \\
&\quad = \sqrt{5} \sum_L \mathrm{i}^L (2L+1) j_L(k\chi_*) \sum_{\ell,m,s} (-1)^\ell \sqrt{2\ell+1} (-1)^{2+L+\ell} \begin{pmatrix} 2 & L & \ell \\ -p & 0 & m \end{pmatrix} \begin{pmatrix} 2 & L & \ell \\ \pm 2 & 0 & -s \end{pmatrix} (-1)^{-s-m}\, {}_s Y_{\ell m}(\mathbf{e}) \\
&\quad = \sqrt{5} \sum_L (-\mathrm{i})^L (2L+1) j_L(k\chi_*) \sum_\ell \sqrt{2\ell+1} \begin{pmatrix} 2 & L & \ell \\ -p & 0 & p \end{pmatrix} \begin{pmatrix} 2 & L & \ell \\ \pm 2 & 0 & \mp 2 \end{pmatrix} {}_{\pm 2}Y_{\ell p}(\mathbf{e})
\end{aligned}
$$

where we have used in the second line the product formula (142) and in the third line the conjugation relation (139) for spin-weighted spherical harmonics (see Appendix F), as well as relabelled $m, s \to -m, -s$ and employed in the third line the time-reversal formula (136) for the Wigner $3j$-symbols (see Appendix E). Furthermore, in the last line the only terms that survive in the m, s summations are $m = p$ and $s = \pm 2$ summands ($Q \pm \mathrm{i}U$ is spin ± 2 and $m = p$ as argued earlier).

We follow a similar procedure to the one in Appendix E. The summation is over $\ell - 2 \leqslant L \leqslant \ell + 2$ by the triangle inequality of the Wigner $3j$-symbols, and we have the results below

$$
\begin{aligned}
\begin{pmatrix} 2 & \ell+2 & \ell \\ \mp 2 & 0 & \pm 2 \end{pmatrix} \begin{pmatrix} 2 & \ell+2 & \ell \\ \pm 2 & 0 & \mp 2 \end{pmatrix} &= \frac{1}{4} \frac{\ell(\ell-1)}{(2\ell+1)(2\ell+3)(2\ell+5)}, \\
\begin{pmatrix} 2 & \ell+1 & \ell \\ \mp 2 & 0 & \pm 2 \end{pmatrix} \begin{pmatrix} 2 & \ell+1 & \ell \\ \pm 2 & 0 & \mp 2 \end{pmatrix} &= \mp \frac{\ell-1}{2(2\ell+1)(2\ell+3)}, \\
\begin{pmatrix} 2 & \ell & \ell \\ \mp 2 & 0 & \pm 2 \end{pmatrix} \begin{pmatrix} 2 & \ell & \ell \\ \pm 2 & 0 & \mp 2 \end{pmatrix} &= \frac{3}{2} \frac{(\ell-1)(\ell+2)}{(2\ell-1)(2\ell+1)(2\ell+3)}, \\
\begin{pmatrix} 2 & \ell-1 & \ell \\ \mp 2 & 0 & \pm 2 \end{pmatrix} \begin{pmatrix} 2 & \ell-1 & \ell \\ \pm 2 & 0 & \mp 2 \end{pmatrix} &= \mp \frac{\ell+2}{2(2\ell-1)(2\ell+1)}, \\
\begin{pmatrix} 2 & \ell-2 & \ell \\ \mp 2 & 0 & \pm 2 \end{pmatrix} \begin{pmatrix} 2 & \ell-2 & \ell \\ \pm 2 & 0 & \mp 2 \end{pmatrix} &= \frac{1}{4} \frac{(\ell+1)(\ell+2)}{(2\ell-3)(2\ell-1)(2\ell+1)}.
\end{aligned}
$$

Hence the sum $\sum_L (-\mathrm{i})^L (2L+1) j_L(x) \begin{pmatrix} 2 & L & \ell \\ -p & 0 & p \end{pmatrix} \begin{pmatrix} 2 & L & \ell \\ \pm 2 & 0 & \mp 2 \end{pmatrix}$ becomes

$$
(-\mathrm{i})^\ell \left\{ \frac{1}{4} \left[-\frac{\ell(\ell-1)}{(2\ell+1)(2\ell+3)} j_{\ell+2} + \frac{6(\ell-1)(\ell+2)}{(2\ell-1)(2\ell+3)} j_\ell - \frac{(\ell+1)(\ell+2)}{(2\ell-1)(2\ell+1)} j_{\ell-2} \right] + \frac{\mathrm{i}}{2} \left(\frac{\ell-1}{2\ell+1} j_{\ell+1} - \frac{\ell+2}{2\ell+1} j_{\ell-1} \right) \right\}.
$$

Now the result (83) can be derived using the following recursion relations for the spherical Bessel functions:

$$
\frac{j_\ell(x)}{x} = \frac{1}{2\ell+1} [j_{\ell-1}(x) + j_{\ell+1}(x)], \quad (2\ell+1) j'_\ell(x) = \ell j_{\ell-1}(x) - (\ell+1) j_{\ell+1}(x)
$$

from which we identify

$$
2\beta_\ell(x) = \frac{1}{2\ell+1} [(\ell+2) j_{\ell-1} - (\ell-1) j_{\ell+1}]
$$

as well as

$$\frac{j'_\ell}{x} = \frac{\ell}{(2\ell+1)(2\ell-1)}(j_{\ell-2}+j_\ell) - \frac{\ell+1}{(2\ell+1)(2\ell+3)}(j_\ell + j_{\ell+2}),$$
$$j''_\ell = \frac{\ell}{2\ell+1}\left(\frac{\ell-1}{2\ell-1}j_{\ell-2} - \frac{\ell}{2\ell-1}j_\ell\right) - \frac{\ell+1}{(2\ell+1)(2\ell+3)}[(\ell+1)j_\ell - (\ell+2)j_{\ell+2}]$$

and Eqn. (137), so that

$$4\epsilon_\ell(x) = \frac{\ell(\ell-1)}{(2\ell+1)(2\ell+3)}j_{\ell+2} - \frac{6(\ell-1)(\ell+2)}{(2\ell-1)(2\ell+3)}j_\ell + \frac{(\ell+1)(\ell+2)}{(2\ell-1)(2\ell+1)}j_{\ell-2}.$$

I. Polarisation from Scalar Perturbations

We prove here that scalar perturbations do not generate B-mode polarisation. Expanding the Fourier transform of $Q \pm \mathrm{i}U$ in normal modes,

$$(Q \pm \mathrm{i}U)(\eta, \mathbf{k}, \mathbf{e}) = \sum_{\ell,m}(-\mathrm{i})^\ell \frac{4\pi}{2\ell+1}(E_\ell \pm \mathrm{i}B_\ell)(\eta,\mathbf{k})Y^*_{\ell m}(\hat{\mathbf{k}})\,{}_{\pm 2}Y_{\ell m}(\mathbf{e}), \tag{146}$$

we substitute this into the Boltzmann equation (79) for linear polarisation. If we take $\mathbf{k} = k\hat{\mathbf{z}}$ then the result is $a + b = c$ where the quantities to be examined separately are

$$a \equiv \sum_{\ell,m}(-\mathrm{i})^\ell \frac{4\pi}{2\ell+1}(\dot{E}_\ell \pm \mathrm{i}\dot{B}_\ell)Y^*_{\ell m}(\hat{\mathbf{k}})\,{}_{\pm 2}Y_{2m}(\mathbf{e}) = \sum_\ell (-\mathrm{i})^\ell \sqrt{\frac{4\pi}{2\ell+1}}(\dot{E}_\ell \pm \mathrm{i}\dot{B}_\ell)Y_{\ell 0}(\hat{\mathbf{e}}),$$

$$\begin{aligned}
b &\equiv \sum_{\ell,m}(-\mathrm{i})^\ell \frac{4\pi}{2\ell+1}\mathrm{i}\mathbf{e}\cdot\mathbf{k}(E_\ell \pm \mathrm{i}B_\ell)Y^*_{\ell m}(\hat{\mathbf{k}})\,{}_{\pm 2}Y_{\ell m}(\mathbf{e}) \\
&= -\sum_{\ell,m}(-\mathrm{i})^{\ell+1}\frac{4\pi}{2\ell+1}k(E_\ell \pm \mathrm{i}B_\ell)Y^*_{\ell m}(\hat{\mathbf{k}})\left[\frac{1}{\ell+1}\sqrt{\frac{[(\ell+1)^2-m^2][(\ell+1)^2-4]}{4(\ell+1)^2-1}}\,{}_{\pm 2}Y_{\ell+1\,m}(\mathbf{e})\right. \\
&\qquad\qquad \left. \mp \frac{2m}{\ell(\ell+1)}\,{}_{\pm 2}Y_{\ell m}(\mathbf{e}) + \frac{1}{\ell}\sqrt{\frac{(\ell^2-m^2)(\ell^2-4)}{4\ell^2-1}}\,{}_{\pm 2}Y_{\ell-1\,m}(\mathbf{e})\right] \\
&= -4\pi k\sum_{\ell,m}(-\mathrm{i})^\ell\left[\frac{1}{2\ell-1}(E_{\ell-1} \pm \mathrm{i}B_{\ell-1})Y^*_{\ell-1\,m}(\hat{\mathbf{k}})\frac{1}{\ell}\sqrt{\frac{(\ell^2-m^2)(\ell^2-4)}{4\ell^2-1}}\,{}_{\pm 2}Y_{\ell m}(\mathbf{e})\right. \\
&\qquad \pm \frac{\mathrm{i}}{2\ell+1}(E_\ell \pm \mathrm{i}B_\ell)Y^*_{\ell m}(\hat{\mathbf{k}})\frac{2m}{\ell(\ell+1)}\,{}_{\pm 2}Y_{\ell m}(\mathbf{e}) \\
&\qquad \left. - \frac{1}{2\ell+3}(E_{\ell+1} \pm \mathrm{i}B_{\ell+1})Y^*_{\ell+1\,m}(\hat{\mathbf{k}})\frac{1}{\ell+1}\sqrt{\frac{[(\ell+1)^2-m^2][(\ell+1)^2-4]}{4(\ell+1)^2-1}}\,{}_{\pm 2}Y_{\ell m}(\mathbf{e})\right] \\
&= -\sqrt{4\pi}k\sum_\ell(-\mathrm{i})^\ell\left[\frac{1}{2\ell-1}\sqrt{\frac{\ell^2-4}{2\ell+1}}(E_{\ell-1} \pm \mathrm{i}B_{\ell-1}) - \frac{1}{2\ell+3}\sqrt{\frac{[(\ell+1)^2-4]}{2\ell+1}}(E_{\ell+1} \pm \mathrm{i}B_{\ell+1})\right]\,{}_{\pm 2}Y_{\ell 0}(\mathbf{e})
\end{aligned}$$

and

$$\begin{aligned}
c &\equiv \sum_{\ell,m}(-\mathrm{i})^\ell \frac{4\pi}{2\ell+1}\dot{\tau}(E_\ell \pm \mathrm{i}B_\ell)Y^*_{\ell m}(\hat{\mathbf{k}})\,{}_{\pm 2}Y_{\ell m}(\mathbf{e}) - \frac{3}{5}\dot{\tau}\sum_{|m|\leqslant 2}\left(E_{2m} - \frac{1}{\sqrt{6}}\Theta_{2m}\right)\,{}_{\pm 2}Y_{2m}(\mathbf{e}) \\
&= \sum_\ell(-\mathrm{i})^\ell\sqrt{\frac{4\pi}{2\ell+1}}\dot{\tau}(E_\ell \pm \mathrm{i}B_\ell)\,{}_{\pm 2}Y_{\ell 0}(\mathbf{e}) - \frac{3}{5}\dot{\tau}\sum_\ell \delta_{\ell 2}\sum_{|m|\leqslant 2}\left(E_{\ell m} - \frac{1}{\sqrt{6}}\Theta_{\ell m}\right)\,{}_{\pm 2}Y_{\ell m}(\mathbf{e}).
\end{aligned}$$

The following results have been used in the derivation above: 1) $Y^*_{\ell m}(\hat{\mathbf{z}}) = \sqrt{(2\ell+1)/(4\pi)}\delta_{m0}$; 2) the recursion relation

$$\cos\theta\, {}_sY_{\ell m} = \frac{1}{\ell+1}\sqrt{\frac{[(\ell+1)^2-m^2][(\ell+1)^2-s^2]}{4(\ell+1)^2-1}}\, {}_sY_{\ell+1\, m} - \frac{sm}{\ell(\ell+1)}\, {}_sY_{\ell m} + \frac{1}{\ell}\sqrt{\frac{(\ell^2-m^2)(\ell^2-s^2)}{4\ell^2-1}}\, {}_sY_{\ell-1\, m}\,.$$

We have now arrived at

$$\sum_\ell (-\mathrm{i})^\ell \sqrt{\frac{4\pi}{2\ell+1}}\left\{(\dot{E}_\ell \pm \mathrm{i}\dot{B}_\ell) + k\left[\sqrt{\frac{(\ell+1)^2-4}{2\ell+3}}(E_{\ell+1} \pm \mathrm{i}B_{\ell+1}) - \sqrt{\frac{\ell^2-4}{2\ell-1}}(E_{\ell-1} \pm \mathrm{i}B_{\ell-1})\right]\right\}{}_{\pm 2}Y_{\ell 0}(\mathbf{e})$$
$$= \sum_\ell (-\mathrm{i})^\ell \sqrt{\frac{4\pi}{2\ell+1}}\dot{\tau}(E_\ell \pm \mathrm{i}B_\ell)\,{}_{\pm 2}Y_{\ell 0}(\mathbf{e}) - \frac{3}{5}\dot{\tau}\sum_\ell \delta_{\ell 2}\sum_{|m|\leqslant 2}\left(E_{\ell m} - \frac{1}{\sqrt{6}}\Theta_{\ell m}\right){}_{\pm 2}Y_{\ell m}(\mathbf{e}). \quad (147)$$

Adding and subtracting this equation with different ± signs, we obtain

$$\dot{E}_\ell + k\left[\sqrt{\frac{(\ell+1)^2-4}{2\ell+3}}E_{\ell+1} - \sqrt{\frac{\ell^2-4}{2\ell-1}}E_{\ell-1}\right] = \dot{\tau}\left[E_\ell - \frac{3}{5}\delta_{\ell 2}\left(E_2 - \frac{1}{\sqrt{6}}\Theta_2\right)\right],$$
$$\dot{B}_\ell + k\left[\sqrt{\frac{(\ell+1)^2-4}{2\ell+3}}B_{\ell+1} - \sqrt{\frac{\ell^2-4}{2\ell-1}}B_{\ell-1}\right] = \dot{\tau}B_\ell.$$